Formation of large-scale semiorganized structures in turbulent convection

Tov Elperin,* Nathan Kleeorin,† and Igor Rogachevskii‡
Department of Mechanical Engineering, The Ben-Gurion University of the Negev, POB 653, Beer-Sheva 84105, Israel

Sergej Zilitinkevich§
Department of Earth Sciences, Meteorology, Uppsala University, Villavagen 16, S-752 36 Uppsala, Sweden
(Received 29 July 2002; published 19 December 2002)

A new mean-field theory of turbulent convection is developed by considering only the small-scale part of spectra as ''turbulence'' and the large-scale part, as a ''mean flow,'' which includes both regular and semiorganized motions. The developed theory predicts the convective wind instability in a shear-free turbulent convection. This instability causes formation of large-scale semiorganized fluid motions in the form of cells. Spatial characteristics of these motions, such as the minimum size of the growing perturbations and the size of perturbations with the maximum growth rate, are determined. This study predicts also the existence of the convective shear instability in a sheared turbulent convection. This instability causes formation of large-scale rolls and generation of convective shear waves which have a nonzero hydrodynamic helicity. Increase of shear promotes excitation of the convective shear instability. Applications of the obtained results to the atmospheric turbulent convection and the laboratory experiments on turbulent convection are discussed.

DOI: 10.1103/PhysRevE.66.066305 PACS number(s): 47.27.Te, 47.27.Nz

I. INTRODUCTION

In the last decades it has been recognized that the very high Rayleigh number convective boundary layer (CBL) has more complex nature than might be reckoned. Besides the fully organized component naturally considered as the mean flow and the chaotic small-scale turbulent fluctuations, one more type of motion has been discovered, namely, long-lived large-scale structures, which are neither turbulent nor deterministic (see, e.g., Refs. [1–14]). These semiorganized structures considerably enhance the vertical transports and render them essentially nonlocal in nature. In the atmospheric shear-free convection, the structures represent three-dimensional Benard-type cells composed of narrow uprising plumes and wide downdraughts. They embrace the entire convective boundary layer (~ 2 km in height) and include pronounced large-scale (~ 5 km in diameter) convergence flow patterns close to the surface (see, e.g., Refs. [1,2], and references therein). In sheared convection, the structures represent CBL-scale rolls stretched along the mean wind. Life times of the semiorganized structures are much larger than the turbulent time scales. Thus, these structures can be treated as comparatively stable, quasistationary motions, playing the same role with respect to small-scale turbulence as the mean flow.

In a laboratory turbulent convection several organized features of motion, such as plumes, jets, and the large-scale circulation, are known to exist. The experimentally observed large-scale circulation in the closed box with a heated bottom wall (the Rayleigh-Benard apparatus) is often called the ''mean wind'' (see, e.g., Refs. [15–22], and references therein). There are several unsolved theoretical questions concerning these flows, e.g., how do they arise, and what are their characteristics and dynamics.

In spite of a number of studies, the nature of large-scale semiorganized structures is poorly understood. The Rayleigh numbers Ra based on the molecular transport coefficients are very large (of the order of $10^{11}-10^{13}$). This corresponds to fully developed turbulent convection in atmospheric and laboratory flows. At the same time the effective Rayleigh numbers $\mathrm{Ra}^{(\mathrm{eff})}$ based on the turbulent transport coefficients (the turbulent viscosity and turbulent diffusivity) are not high, e.g., $\mathrm{Ra}^{(\mathrm{eff})} \sim \mathrm{Ra}/(\mathrm{RePe})$, where Re and Pe are the Reynolds and Peclet numbers, respectively. They are less than the critical Rayleigh numbers required for the excitation of large-scale convection. Hence the emergence of large-scale convective flows (which are observed in the atmospheric and laboratory flows) seems puzzling.

The main goal of this study is to suggest a mechanism for excitation of large-scale circulations (large-scale convection). In particular, in the present paper we develop a new mean-field theory of turbulent convection by considering only the small-scale part of spectra as turbulence and the large-scale part, as a mean flow, which includes both, regular and semiorganized motions. We found a convective wind instability in a shear-free turbulent convection which results in the formation of large-scale semiorganized fluid motions in the form of cells (convective wind). We determined the spatial characteristics of these motions, such as the minimum size of the growing perturbations and the size of perturbations with the maximum growth rate. In addition, we studied a convective shear instability in a sheared turbulent convection which causes formation of large-scale rolls and a generation of convective shear waves. We analyzed the relevance of the obtained results to the turbulent convection in the atmosphere and the laboratory experiments.

Traditional theoretical models of the boundary-layer tur-

*Electronic address: elperin@menix.bgu.ac.il
URL: http://www.bgu.ac.il/~elperin
†Electronic address: nat@menix.bgu.ac.il
‡Electronic address: gary@menix.bgu.ac.il
URL: http://www.bgu.ac.il/~gary
§Electronic address: sergej@met.uu.se

bulence, such as the Kolmogorov-type closures and similarity theories (e.g., the Monin-Obukhov surface-layer similarity theory) imply two assumptions: (i) Turbulent flows can be decomposed into two components of principally different nature: fully organized (mean flow) and fully turbulent flows. (ii) Turbulent fluxes are uniquely determined by the local mean gradients. For example, the turbulent flux of entropy is given by

$$\langle s\mathbf{u}\rangle = -\kappa_T \boldsymbol{\nabla}\overline{S} \tag{1}$$

(see, e.g., Ref. [23]), where κ_T is the turbulent thermal conductivity, $\overline{S}$ is the mean entropy, $\mathbf{u}$ and s are fluctuations of the velocity and entropy.

However, the mean-velocity gradients can affect the turbulent flux of entropy. The reason is that additional, essentially nonisotropic velocity fluctuations can be generated by tangling of the mean-velocity gradients with the Kolmogorov-type turbulence. The source of energy of this ''tangling turbulence'' is the energy of the Kolmogorov turbulence.

In the present paper we showed that the tangling turbulence can cause formation of semiorganized structures due to excitation of large-scale instability. The tangling turbulence was introduced by Wheelon [24] and Batchelor *et al.* [25] for a passive scalar and by Golitsyn [26] and Moffatt [27] for a passive vector (magnetic field). Anisotropic fluctuations of a passive scalar (e.g., the number density of particles or temperature) are generated by tangling of gradients of the mean passive scalar field with random velocity field. Similarly, anisotropic magnetic fluctuations are excited by tangling of the mean magnetic field with the velocity fluctuations. The Reynolds stresses in a turbulent flow with a mean-velocity shear is another example of a tangling turbulence. Indeed, they are strongly anisotropic in the presence of shear and have a steeper spectrum ($\propto k^{-7/3}$) than a Kolmogorov turbulence (see, e.g., Refs. [28–31]). The anisotropic velocity fluctuations of tangling turbulence were studied first by Lumley [28].

This paper is organized as follows. In Sec. II we described the governing equations and the method of the derivations of the turbulent flux of entropy and Reynolds stresses. In Sec. III using the derived mean-field equations we studied the large-scale instability in a shear-free turbulent convection which causes formation of semiorganized fluid motions in the form of cells. In Sec. IV the instability in a sheared turbulent convection is investigated and the formation of large-scale semiorganized rolls is described. Application of the obtained results for the analysis of observed semiorganized structures in the atmospheric turbulent convection is discussed in Sec. V.

II. THE GOVERNING EQUATIONS AND THE METHOD OF THE DERIVATIONS

Our goal is to study the tangling turbulence, in particular, an effect of sheared large-scale motions on a developed turbulent stratified convection. To this end we consider a fully developed turbulent convection in a stratified nonrotating fluid with large Rayleigh and Reynolds numbers. The governing equations read

$$\left(\frac{\partial}{\partial t}+\mathbf{v}\cdot\boldsymbol{\nabla}\right)\mathbf{v} = -\boldsymbol{\nabla}\left(\frac{P}{\rho_0}\right) - \mathbf{g}S + \mathbf{f}_\nu(\mathbf{v}), \tag{2}$$

$$\left(\frac{\partial}{\partial t}+\mathbf{v}\cdot\boldsymbol{\nabla}\right)S = -\mathbf{v}\cdot\mathbf{N}_b - \frac{1}{T_0}\boldsymbol{\nabla}\cdot\mathbf{F}_\kappa(S), \tag{3}$$

where $\mathbf{v}$ is the fluid velocity with $\boldsymbol{\nabla}\cdot\mathbf{v}=\boldsymbol{\Lambda}\cdot\mathbf{v}$, $\mathbf{g}$ is the acceleration of gravity, $\rho_0\mathbf{f}_\nu(\mathbf{v})$ is the viscous force, $\mathbf{F}_\kappa(S)$ is the heat flux that is associated with the molecular heat conductivity κ, $\boldsymbol{\Lambda}=-\rho_0^{-1}\boldsymbol{\nabla}\rho_0$ is the density stratification scale, and $\mathbf{N}_b=(\gamma P_0)^{-1}\boldsymbol{\nabla}P_0-\rho_0^{-1}\boldsymbol{\nabla}\rho_0$. The variables with the subscript ''0'' correspond to the hydrostatic equilibrium $\boldsymbol{\nabla}P_0=\rho_0\mathbf{g}$, and T_0 is the equilibrium fluid temperature, $S=P/\gamma P_0-\rho/\rho_0$ are the deviations of the entropy from the hydrostatic equilibrium value, P and ρ are the deviations of the fluid pressure and density from the hydrostatic equilibrium. Note that the variable $S=\Theta/\Theta_0$, where Θ is the potential temperature which is used in atmospheric physics. The Brunt-Väisälä frequency Ω_b is determined by the equation $\Omega_b^2=-\mathbf{g}\cdot\mathbf{N}_b$. In order to derive Eq. (2) we used an identity: $-\boldsymbol{\nabla}P+\mathbf{g}\rho=-\rho_0[\boldsymbol{\nabla}(P/\rho_0)+\mathbf{g}S-P\mathbf{N}_b/\rho_0]$, where we assumed that $|P\mathbf{N}_b/\rho_0|\ll|\mathbf{g}S|$ and $|P\mathbf{N}_b/\rho_0|\ll|\boldsymbol{\nabla}(P/\rho_0)|$. This assumption corresponds to a nearly isentropic basic reference state when $\mathbf{N}_b$ is very small. For the derivation of this identity we also used the equation for the hydrostatic equilibrium. Equations (2) and (3) are written in the Boussinesq approximation for $\boldsymbol{\nabla}\cdot\mathbf{v}\neq 0$.

A. Mean-field approach

We use a mean-field approach whereby the velocity, pressure, and entropy are separated into the mean and fluctuating parts: $\mathbf{v}=\overline{\mathbf{U}}+\mathbf{u}$, $P=\overline{P}+p$, and $S=\overline{S}+s$, the fluctuating parts have zero mean values, $\overline{\mathbf{U}}=\langle\mathbf{v}\rangle$, $\overline{P}=\langle P\rangle$ and $\overline{S}=\langle S\rangle$. Averaging Eqs. (2) and (3) over an ensemble of fluctuations we obtain the mean-field equations

$$\left(\frac{\partial}{\partial t}+\overline{\mathbf{U}}\cdot\boldsymbol{\nabla}\right)\overline{U}_i = -\nabla_i\left(\frac{\overline{P}}{\rho_0}\right)+(\Lambda_j-\nabla_j)\langle u_i u_j\rangle - \mathbf{g}\overline{S}+\overline{\mathbf{f}}_\nu(\overline{\mathbf{U}}), \tag{4}$$

$$\left(\frac{\partial}{\partial t}+\overline{\mathbf{U}}\cdot\boldsymbol{\nabla}\right)\overline{S} = -\overline{\mathbf{U}}\cdot\mathbf{N}_b+(\Lambda_i-\nabla_i)\langle s\,u_i\rangle - \frac{1}{T_0}\boldsymbol{\nabla}\cdot\overline{\mathbf{F}}_\kappa(\overline{\mathbf{U}},\overline{S}), \tag{5}$$

where $\rho_0\overline{\mathbf{f}}_\nu(\overline{\mathbf{U}})$ is the mean molecular viscous force, $\overline{\mathbf{F}}_\kappa(\overline{\mathbf{U}},\overline{S})$ is the mean heat flux that is associated with the molecular thermal conductivity. In order to derive a closed system of the mean-field equations we have to determine the mean-field dependencies of the Reynolds stresses $f_{ij}(\overline{\mathbf{U}},\overline{S})=\langle u_i(t,\mathbf{x})u_j(t,\mathbf{x})\rangle$ and the flux of entropy $\Phi_i(\overline{\mathbf{U}},\overline{S})=\langle s(t,\mathbf{x})u_i(t,\mathbf{x})\rangle$. To this end we used equations for the fluctuations $\mathbf{u}(t,\mathbf{r})$ and $s(t,\mathbf{r})$ which are obtained by subtracting Eqs. (4) and (5) for the mean fields from the corresponding Eqs. (2) and (3) for the total fields,

$$\frac{\partial \mathbf{u}}{\partial t} = -(\overline{\mathbf{U}}\cdot\boldsymbol{\nabla})\mathbf{u} - (\mathbf{u}\cdot\boldsymbol{\nabla})\overline{\mathbf{U}} - \boldsymbol{\nabla}\left(\frac{p}{\rho_0}\right) - \mathbf{g}\,s + \mathbf{U}_N, \quad (6)$$

$$\frac{\partial s}{\partial t} = -\mathbf{u}\cdot(\mathbf{N}_b + \boldsymbol{\nabla}\overline{S}) - (\overline{\mathbf{U}}\cdot\boldsymbol{\nabla})s + S_N, \quad (7)$$

where $U_N = \langle(\mathbf{u}\cdot\boldsymbol{\nabla})\mathbf{u}\rangle - (\mathbf{u}\cdot\boldsymbol{\nabla})\mathbf{u} + \mathbf{f}_\nu(\mathbf{u})$ and $S_N = \langle(\mathbf{u}\cdot\boldsymbol{\nabla})s\rangle - (\mathbf{u}\cdot\boldsymbol{\nabla})s - (1/T_0)\boldsymbol{\nabla}\cdot\mathbf{F}_\kappa(\mathbf{u},s)$ are the nonlinear terms which include the molecular dissipative terms.

B. Method of derivations

By means of Eqs. (6) and (7) we determined the dependencies of the second moments $f_{ij}(\overline{\mathbf{U}},\overline{S})$ and $\Phi_i(\overline{\mathbf{U}},\overline{S})$ on the mean fields $\overline{\mathbf{U}}$ and $\overline{S}$. The procedure of the derivation is outlined in the following (for details see Appendix A).

(a) Using Eqs. (6) and (7) we derived equations for the following second moments:

$$f_{ij}(\mathbf{k}) = \hat{L}(u_i,u_j), \quad \Phi_i(\mathbf{k}) = \hat{L}(s,u_i), \quad (8)$$

$$F(\mathbf{k}) = \hat{L}(s,\omega), \quad G(\mathbf{k}) = \hat{L}(\omega,\omega), \quad (9)$$

$$H(\mathbf{k}) = \hat{L}(s,s), \quad (10)$$

where $\hat{L}(a,b) = \langle a(\mathbf{k})b(-\mathbf{k})\rangle$, $\omega = (\boldsymbol{\nabla}\times\mathbf{u})_z$, the acceleration of gravity $\mathbf{g}$ is directed opposite to the z axis. Here we used a two-scale approach. This implies that we assumed that there exists a separation of scales, i.e., the maximum scale of turbulent motions l_0 is much smaller than the characteristic scale of inhomogeneities of the mean fields. Our final results showed that this assumption is indeed valid. The equations for the second moments (8)–(10) are given by Eqs. (A15), (A16), and (A21)–(A23) in Appendix A. In the derivation we assumed that the inverse density stratification scale $\Lambda^2 \ll k^2$.

(b) The derived equations for the second moments contain the third moments, and a problem of closing the equations for the higher moments arises. Various approximate methods have been proposed for the solution of problems of this type (see, e.g., [23,32,33]). The simplest procedure is the τ approximation which was widely used for study of different problems of turbulent transport (see, e.g., [32,34–36]). One of the simplest procedures that allows us to express the third moments f_{ij}^N, $\boldsymbol{\Phi}^N$, . . . , H_N in Eqs. (A15), (A16), and (A23) in terms of the second moments, reads

$$A_N(\mathbf{k}) - A_N^{(0)}(\mathbf{k}) = -\frac{A(\mathbf{k}) - A^{(0)}(\mathbf{k})}{\tau(k)}, \quad (11)$$

where the superscript (0) corresponds to the background turbulent convection (i.e., a turbulent convection with $\nabla_i\overline{U}_j = 0$), and $\tau(k)$ is the characteristic relaxation time of the statistical moments. Note that we applied τ approximation (11) only to study the deviations from the background turbulent convection which are caused by the spatial derivatives of the mean velocity. The background turbulent convection is assumed to be known.

The τ approximation is in general similar to Eddy damped quasinormal Markowian (EDQNM) approximation. However, there is a principle difference between these two approaches (see Refs. [32,33]). The EDQNM closures do not relax to the equilibrium, and this procedure does not describe properly the motions in the equilibrium state. Within the EDQNM theory, there is no dynamically determined relaxation time, and no slightly perturbed steady state can be approached [32]. In the τ approximation, the relaxation time for small departures from equilibrium is determined by the random motions in the equilibrium state, but not by the departure from equilibrium [32]. Analysis performed in Ref. [32] showed that the τ approximation describes the relaxation to the equilibrium state (the background turbulent convection) more accurately than the EDQNM approach.

(c) We assumed that the characteristic times of variation of the second moments $f_{ij}(\mathbf{k})$, $\Phi_i(\mathbf{k})$, . . . , $H(\mathbf{k})$ are substantially larger than the correlation time $\tau(k)$ for all turbulence scales. This allowed us to determine a stationary solution for the second moments $f_{ij}(\mathbf{k})$, $\Phi_i(\mathbf{k})$, . . . , $H(\mathbf{k})$.

(d) For the integration in $\mathbf{k}$ space of the second moments $f_{ij}(\mathbf{k})$, $\Phi_i(\mathbf{k})$, . . . , $H(\mathbf{k})$ we have to specify a model for the background turbulent convection. Here we used the following model of the background turbulent convection which is discussed in more details in Appendix B:

$$f_{ij}^{(0)}(\mathbf{k}) = f_*[P_{ij}(\mathbf{k}) + \varepsilon P_{ij}^{(\perp)}(\mathbf{k}_\perp)]\widetilde{W}(k), \quad (12)$$

$$\Phi_i^{(0)}(\mathbf{k}) = k_\perp^{-2}[k^2\Phi_z^{(0)}(\mathbf{k})e_jP_{ij}(\mathbf{k}) + iF^{(0)}(\mathbf{k})(\mathbf{e}\times\mathbf{k})_i], \quad (13)$$

$$\Phi_z^{(0)}(\mathbf{k}) = \Phi_z^*\left[2\alpha - 3(\alpha-1)\left(\frac{k_\perp}{k}\right)^2\right]\widetilde{W}(k), \quad (14)$$

$$F^{(0)}(\mathbf{k}) = -6if^{(0)}(\mathbf{k})[\boldsymbol{\Phi}^*\cdot(\mathbf{e}\times\mathbf{k})], \quad (15)$$

$$G^{(0)}(\mathbf{k}) = (1+\varepsilon)f_*f^{(0)}(\mathbf{k})k^2, \quad (16)$$

$$H^{(0)}(\mathbf{k}) = 2H_*\widetilde{W}(k), \quad (17)$$

where $\widetilde{W}(k) = W(k)/8\pi k^2$, $f^{(0)}(\mathbf{k}) = (k_\perp/k)^2\widetilde{W}(k)$, $\varepsilon = (2/3)[\langle\mathbf{u}_\perp^2\rangle/\langle\mathbf{u}_z^2\rangle - 2]$ is the degree of anisotropy of the turbulent velocity field $\mathbf{u} = \mathbf{u}_\perp + u_z\mathbf{e}$, α is the degree of anisotropy of the turbulent flux of entropy (see below and Appendix B), $P_{ij}(\mathbf{k}) = \delta_{ij} - k_{ij}$, $k_{ij} = k_ik_j/k^2$, $\mathbf{k} = \mathbf{k}_\perp + k_z\mathbf{e}$, $k_z = \mathbf{k}\cdot\mathbf{e}$, $P_{ij}^{(\perp)}(\mathbf{k}_\perp) = \delta_{ij} - k_{ij}^\perp - e_{ij}$, $k_{ij}^\perp = (\mathbf{k}_\perp)_i(\mathbf{k}_\perp)_j/k_\perp^2$, $e_{ij} = e_ie_j$, $\mathbf{e}$ is the unit vector directed along the z axis. Here $\tau(k) = 2\tau_0\overline{\tau}(k)$, $W(k) = -d\overline{\tau}(k)/dk$, $\overline{\tau}(k) = (k/k_0)^{1-q}$, $1 < q < 3$ is the exponent of the kinetic energy spectrum ($q = 5/3$ for Kolmogorov spectrum), $k_0 = 1/l_0$, and l_0 is the maximum scale of turbulent motions, $\tau_0 = l_0/u_0$ and u_0 is the characteristic turbulent velocity in the scale l_0. Motion in the background turbulent convection is assumed to be nonhelical. In Eqs. (12) and (13) we neglected small terms $\sim O(\Lambda f_*; \boldsymbol{\nabla} f_*)$ and $\sim O(\Lambda\Phi^*; \boldsymbol{\nabla}\Phi^*)$, respectively. Note that $f_{ij}^{(0)}(\mathbf{k})e_{ij} = f_*f^{(0)}(\mathbf{k})$. Now we calculate $f_{ij}^{(0)} \equiv \int f_{ij}^{(0)}(\mathbf{k})d\mathbf{k}$ using Eq. (12),

$$f_{ij}^{(0)}=f_*\left[\frac{1}{3}\delta_{ij}+\frac{\varepsilon}{4}(\delta_{ij}-e_{ij})\right]. \tag{18}$$

Note that $\mathbf{\Phi}^{(0)}\equiv\int\mathbf{\Phi}^{(0)}(\mathbf{k})d\mathbf{k}=\mathbf{\Phi}^*$. The parameter α can be presented in the form

$$\alpha=\frac{1+\xi(q+1)/(q-1)}{1+\xi/3}, \tag{19}$$

$$\xi=(l_\perp/l_z)^{q-1}-1, \tag{20}$$

where $l_\perp$ and l_z are the horizontal and vertical scales in which the correlation function $\Phi_z^{(0)}(\mathbf{r})=\langle s(\mathbf{x})\mathbf{u}(\mathbf{x}+\mathbf{r})\rangle$ tends to zero (see Appendix B). The parameter ξ describes the degree of thermal anisotropy. In particular, when $l_\perp=l_z$ the parameter $\xi=0$ and $\alpha=1$. For $l_\perp\ll l_z$ the parameter $\xi=-1$ and $\alpha=-3/(q-1)$. The maximum value $\xi_{\max}$ of the parameter ξ is given by $\xi_{\max}=q-1$ for $\alpha=3$. Thus, for $\alpha<1$ the thermal structures have the form of column or thermal jets ($l_\perp<l_z$), and for $\alpha>1$ there exist the "pancake" thermal structures ($l_\perp>l_z$) in the background turbulent convection. For statistically stationary small-scale turbulence the degree of anisotropy of turbulent velocity field varies in the range

$$-\min\left\{\frac{4(q+3)}{5(q+1)};\frac{2(19-q)}{25};\frac{4}{3}\right\}<\varepsilon<\infty. \tag{21}$$

The negative (positive) degree of anisotropy ε of a turbulent velocity field corresponds to that the vertical size of turbulent eddies in the background turbulent convection is larger (smaller) than the horizontal size.

(e) In order to determine values f_*, $\mathbf{\Phi}^*$, and H_* in the background turbulent convection we used balance equations (A5)–(A7) for the second moments (see Appendix A).

C. Turbulent flux of entropy

The procedure described in this section allows us to determine the Reynolds stresses and turbulent flux of entropy which are given by Eqs. (A33) and (A34) in Appendix A, where we considered the case $\nabla\cdot\overline{\mathbf{U}}=\mathbf{0}$. In particular, the formula for turbulent flux of entropy reads

$$\mathbf{\Phi}-\mathbf{\Phi}^*=[-5\alpha(\nabla\cdot\overline{\mathbf{U}}_\perp)\mathbf{\Phi}_\parallel^*+(\alpha+3/2)(\overline{\boldsymbol{\omega}}\times\mathbf{\Phi}_\parallel^*)+3(\overline{\boldsymbol{\omega}}_\parallel\times\mathbf{\Phi}^*)]\frac{\tau_0(q+1)}{15}+(\nabla\times\mathbf{T})+(\mathbf{E}\cdot\nabla)\overline{\mathbf{U}}, \tag{22}$$

where $\overline{\omega}=(\nabla\times\overline{\mathbf{U}})_z$, $\mathbf{\Phi}_\parallel^*=\Phi_z^*\mathbf{e}$, $\overline{\boldsymbol{\omega}}_\parallel=\overline{\omega}\mathbf{e}$, $\mathbf{T}=(2/5)\tau_0(q-2)[\mathbf{\Phi}^*\cdot(\mathbf{e}\times\overline{\mathbf{U}})]$ and $\mathbf{E}=(1/5)\tau_0\{[2-q-2\alpha(q+1)/3]\mathbf{\Phi}_\parallel^*-3\mathbf{\Phi}^*\}$. It is shown below that the first and the second terms in Eq. (22) are responsible for the large-scale convective wind instability in a shear-free turbulent convection (see Sec. IV), while the third term in the turbulent flux of entropy (22) causes the convective shear instability (see Sec. V).

The turbulent flux of entropy can be obtained even from simple symmetry reasoning. Indeed, this flux can be presented as a sum of two terms: $\langle s\omega_i\rangle=\Phi_i^*+\beta_{ijk}\nabla_j\overline{U}_k$, where $\mathbf{\Phi}^*$ determines the contribution of the Kolmogorov turbulence and it is independent of $\nabla_i\overline{U}_j$, whereas the second term is proportional to $\nabla_i\overline{U}_j$ and describes the contribution of the tangling turbulence. Here β_{ijk} is an arbitrary true tensor and $\overline{\mathbf{U}}$ is the mean velocity. Using the identity $\nabla_j\overline{U}_i=(\delta\overline{\mathbf{U}})_{ij}-(1/2)\varepsilon_{ijk}\overline{\omega}_k$, the turbulent flux of entropy becomes

$$\langle su_i\rangle=\Phi_i^*+\eta_{ij}\overline{\omega}_j+(\overline{\boldsymbol{\omega}}\times\boldsymbol{\delta})_i+\mu_{ijk}(\delta\overline{\mathbf{U}})_{jk}, \tag{23}$$

where $(\delta\overline{\mathbf{U}})_{ij}=(\nabla_i\overline{U}_j+\nabla_j\overline{U}_i)/2$, $\overline{\boldsymbol{\omega}}=\nabla\times\overline{\mathbf{U}}$ is the mean vorticity, and ε_{ijk} is the fully antisymmetric Levi-Civita tensor. In Eq. (23), η_{ij} is a symmetric pseudotensor, $\boldsymbol{\delta}$ is a true vector, μ_{ijk} is a true tensor symmetric in the last two indexes, $\mathbf{\Phi}\equiv\langle s\mathbf{u}\rangle$ and $\mathbf{\Phi}^*$ are true vectors. The tensors η_{ij}, μ_{ijk} and the vector $\boldsymbol{\delta}$ can be constructed using two vectors: $\mathbf{\Phi}^*$ and the vertical unit vector $\mathbf{e}$. For example, $\eta_{ij}=0$, $\boldsymbol{\delta}=A_1\mathbf{\Phi}^*+A_2\Phi_z^*\mathbf{e}$, and $\mu_{ijk}=A_3\Phi_z^*e_{ijk}+A_4\Phi_i^*e_{jk}$, where A_k are the unknown coefficients and $e_{ijk}=e_ie_je_k$. This yields the following expression for the turbulent flux of entropy in a divergence-free mean-velocity field:

$$\mathbf{\Phi}=\mathbf{\Phi}^*-(A_3+A_4)(\nabla\cdot\overline{\mathbf{U}}_\perp)\mathbf{\Phi}_\parallel^*+(A_1+A_2)(\overline{\boldsymbol{\omega}}\times\mathbf{\Phi}_\parallel^*)+A_1(\overline{\boldsymbol{\omega}}_\parallel\times\mathbf{\Phi}^*)-A_4(\nabla\cdot\overline{\mathbf{U}}_\perp)\mathbf{\Phi}_\perp^*], \tag{24}$$

where $\overline{\mathbf{U}}=\overline{\mathbf{U}}_\perp+\overline{U}_z\mathbf{e}$, $\mathbf{\Phi}_\parallel^*=\Phi_z^*\mathbf{e}$ and $\overline{\boldsymbol{\omega}}_\parallel=\overline{\omega}\mathbf{e}$. Equations (22) and (24) coincide if one sets $A_1=\tau_0(q+1)/5$, $A_2=\tau_0(q+1)(\alpha-3/2)/15$, $A_3=\tau_0\alpha(q+1)/3$, and $A_4=0$. Note that $\mathbf{\Phi}^*=-\kappa_T\nabla\overline{S}-\tau_0\Phi_z^*[d\overline{\mathbf{U}}^{(0)}(z)/dz]$, $\overline{\mathbf{U}}^{(0)}(z)$ is the imposed horizontal large-scale flow velocity (e.g., a wind velocity).

III. CONVECTIVE WIND INSTABILITY IN A SHEAR-FREE TURBULENT CONVECTION

In this section we studied the mean-field dynamics for a shear-free turbulent convection. We showed that under certain conditions a large-scale instability is excited, which causes the formation of large-scale semiorganized structures in a turbulent convection.

The mean-field dynamics is determined by Eqs. (4) and (5). To study the linear stage of an instability we derived linearized equations for the small perturbations from the equilibrium, $\overline{U}_z^{(1)}=\overline{U}_z-\overline{U}_z^{(\mathrm{eq})}$, $\overline{\omega}^{(1)}=\overline{\omega}-\overline{\omega}^{(\mathrm{eq})}$, and $\overline{S}^{(1)}=\overline{S}-\overline{S}^{(\mathrm{eq})}$,

$$\Delta\frac{\partial\overline{U}_z^{(1)}}{\partial t}=\frac{\partial}{\partial z}(\nabla_i\nabla_j f_{ij}^{(1)})-\Delta(e_i\nabla_j f_{ij}^{(1)})+g\Delta_\perp\overline{S}^{(1)}, \tag{25}$$

$$\frac{\partial\overline{\omega}^{(1)}}{\partial t}=-(\mathbf{e}\times\nabla)_i\left[\nabla_j f_{ij}^{(1)}+\frac{\partial\overline{U}_i^{(\mathrm{eq})}}{\partial z}\overline{U}_z^{(1)}\right], \tag{26}$$

$$\frac{\partial \overline{S}^{(1)}}{\partial t} = -(\boldsymbol{\nabla}\cdot\boldsymbol{\Phi}^{(1)}) - \left(N_b + \frac{\partial \overline{S}^{(\mathrm{eq})}}{\partial z}\right)\overline{U}_z^{(1)}, \tag{27}$$

where $f_{ij}^{(1)} = f_{ij} - f_{ij}^{(0)}$ and the Reynolds stresses f_{ij} are given by Eqs. (A33) in Appendix A, $\Delta_\perp = \Delta - \partial^2/\partial z^2$, $\mathbf{N}_b = N_b\mathbf{e}$ and

$$\boldsymbol{\nabla}\cdot\boldsymbol{\Phi}^{(1)} = -(\tau_0/30)(q+1)\{(\boldsymbol{\Phi}^*\cdot\mathbf{e})[10\alpha\Delta_\perp - (8\alpha - 3)\Delta]\overline{U}_z^{(1)} + 6[(\boldsymbol{\Phi}^*\times\mathbf{e})\cdot\boldsymbol{\nabla}]\overline{\omega}^{(1)}\} - \kappa_{ij}\nabla_i\nabla_j\overline{S}^{(1)}, \tag{28}$$

$$\kappa_{ij} = \tau_0\delta_*[f_{ij}^{(0)} + (1/2)g\tau_0\delta_*(4-\gamma)(e_i\Phi_j^* + e_j\Phi_i^*)]. \tag{29}$$

Equation (29) follows from Eqs. (A6) and (A7).

A. The growth rate of convective wind instability

Let us consider a shear-free turbulent convection ($\nabla_i\overline{U}_j^{(0)} = 0$) with a given vertical flux of entropy $\Phi_z^{(\mathrm{eq})}\mathbf{e}$. We also consider an isentropic basic reference state, i.e., we neglect terms which are proportional to $(N_b + \partial\overline{S}^{(\mathrm{eq})}/\partial z)\overline{U}_z^{(1)}$ in Eq. (27). We seek for a solution of Eqs. (25)–(27) in the form $\propto\exp(\gamma_{\mathrm{inst}}t + i\mathbf{K}\cdot\mathbf{R})$, where $\mathbf{K}$ is the wave vector of small perturbations and γ_{inst} is the growth rate of the instability. Thus, the growth rate of the instability is given by

$$\gamma_{\mathrm{inst}} = \nu_T K^2 A[\sqrt{1 + 4B/A^2} - 1]/2, \tag{30}$$

where

$$A = B_1 + B_2, \quad B = \beta X(c_7 - c_8 X) - B_1 B_2, \tag{31}$$

$B_1 = c_1 + c_6 X - c_3 X^2$, $B_2 = c_4 - c_5 X$, $c_1 = (q+3)/5$, $c_3 = \varepsilon(q+3)/4$, $c_4 = \delta_*(2+3\sigma)$, $c_5 = 3\delta_*(\sigma - \varepsilon/2)$, $c_6 = \varepsilon(q+5)/4$, $c_7 = \mu(8\alpha - 3)/10$, $c_8 = \mu\alpha$, with $\sigma = a_*(4-\gamma)(1+\varepsilon/2)$, $\mu = 6a_*(q+1)(1+\varepsilon/2)/\delta_*$, $\beta = (l_0 K)^{-2}$, $X = \sin^2\theta$, $a_* = 2\delta_*\Phi_z^{(\mathrm{eq})} g\tau_0/f_*$, and θ is the angle between $\mathbf{e}$ and the wave vector $\mathbf{K}$ of small perturbations. Here we used that in equilibrium $\Phi_z^{(\mathrm{eq})} = \Phi_z^*$. When $\beta \gg 1$ the growth rate of the instability is given by

$$\gamma_{\mathrm{inst}} \propto \nu_T K^2\sqrt{\mu\beta}\,|\sin\theta|\left[\alpha - \frac{3}{8} - \frac{5\alpha}{4}\sin^2\theta\right]^{1/2} \propto K u_0. \tag{32}$$

Thus for large β the growth rate of the instability is proportional to the wave number K and the instability occurs when $\alpha(5\cos^2\theta - 1) > 3/2$. This yields two ranges for the instability,

$$\frac{3}{2(5\cos^2\theta - 1)} < \alpha < 3, \tag{33}$$

$$-\frac{3}{q-1} < \alpha < -\frac{3}{2(1 - 5\cos^2\theta)}, \tag{34}$$

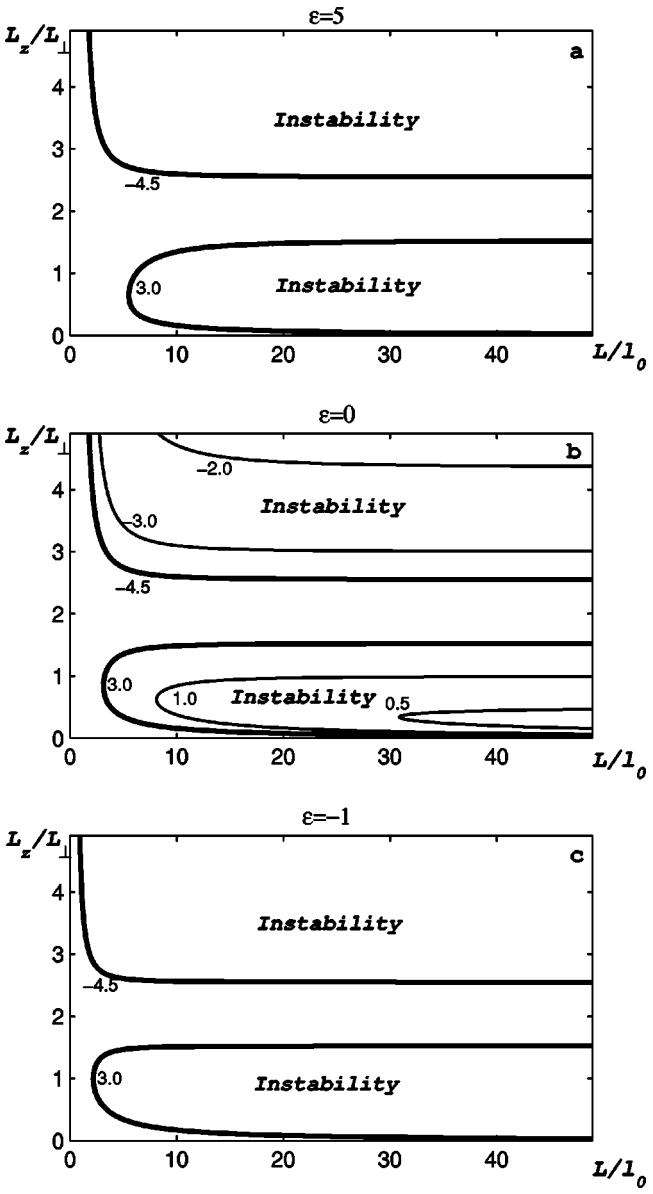

FIG. 1. The range of parameters $(L_z/L_\perp; L/l_0)$ for which the convective wind instability occurs, for different values of the parameter α: (from -4.5 to 3) and for different values of the parameter ε: (a) $\varepsilon = 5$; (b) $\varepsilon = 0$; (c) $\varepsilon = -1$.

where we took into account that the parameter α varies in the interval $-3/(q-1) < \alpha < 3$ (see Appendix B). The first range for the instability in Eq. (33) is for the angles $3/10 \leqslant \cos^2\theta \leqslant 1$ (for $q = 5/3$, the aspect ratio $0 < L_z/L_\perp < 1.53$), and the second range (34) for the instability corresponds to the angles $0 \leqslant \cos^2\theta < (3-q)/10$ (the aspect ratio $2.55 < L_z/L_\perp < \infty$), where $L_z/L_\perp \equiv K_\perp/K_z = \tan\theta$. The conditions (33) and (34) correspond to $\boldsymbol{\nabla}\cdot\boldsymbol{\Phi}^{(1)} < 0$.

Figure 1 demonstrates the range of parameters $L_z/L_\perp$ and L/l_0 where the instability is excited, for different values of the parameter α (from -4.5 to 3) and different values of the parameter $\varepsilon = -1;\ 0;\ 5$. Here $L \equiv 1/\sqrt{L_z^{-2} + L_\perp^{-2}}$ and we assumed that $a_* = 1$. The threshold of the instability L_{cr} depends on the parameter ε. For example, for $\alpha = 3$ the threshold of the instability L_{cr} varies from $3l_0$ to $7l_0$ (when ε changes from -1 to 5). The negative (positive) degree of

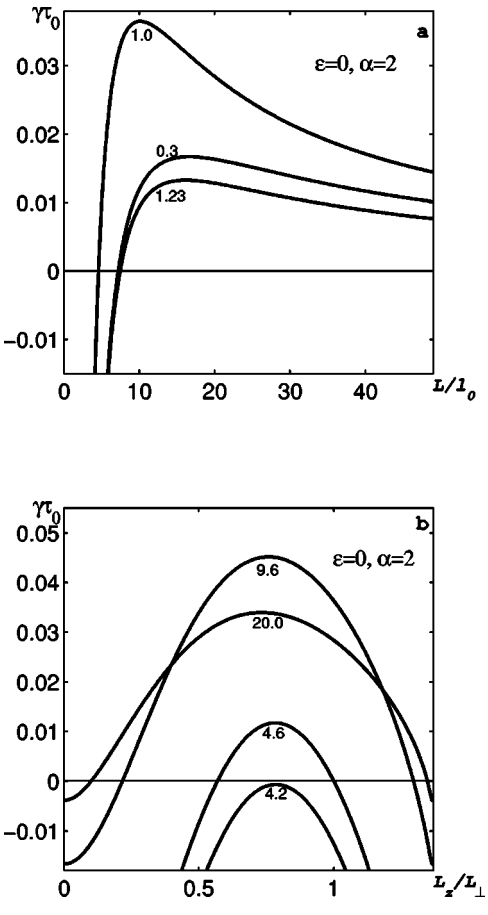

FIG. 2. The growth rate of the convective wind instability as functions of (a) L/l_0 (for different values of parameter $L_z/L_\perp = 0.3;1;1.23$); and (b) $L_z/L_\perp$ (for different values of parameter $L/l_0 = 4.2;4.6;9.6;20$) for $\varepsilon = 0$ and $\alpha = 2$.

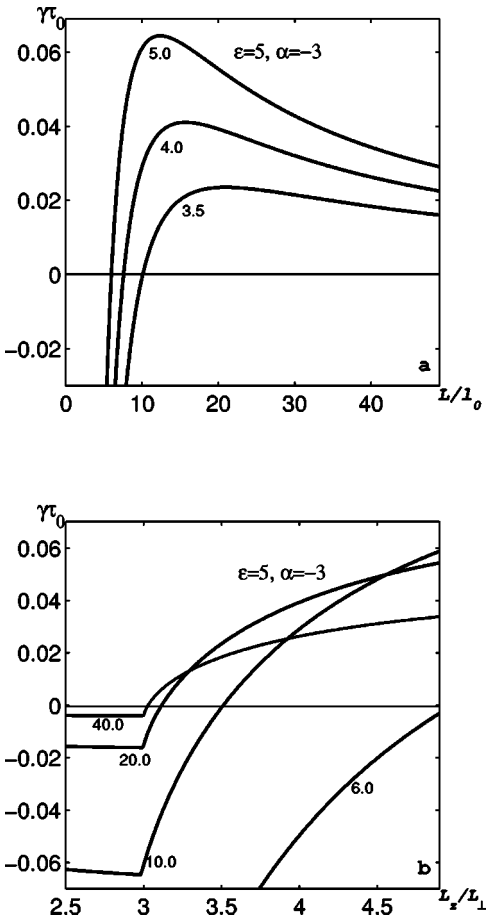

FIG. 3. The growth rate of the convective wind instability as functions of (a) L/l_0 (for different values of parameter $L_z/L_\perp = 3.5;4;5$); and (b) $L_z/L_\perp$ (for different values of parameter $L/l_0 = 6;10;20;40$); for $\varepsilon = 5$ and $\alpha = -3$.

anisotropy ε of turbulent velocity field corresponds to that the vertical size of turbulent eddies in the background turbulent convection is larger (smaller) than the horizontal size. The reason for the increase of the range of instability with the decrease of the degree of anisotropy ε is that the rate of dissipation of the kinetic energy of the mean-velocity field decreases with decrease of ε and it causes decrease of the threshold of the instability. The instability does not occur when $1.53 < L_z/L_\perp < 2.55$ for all ε.

Figure 2 shows the growth rate of the instability as function of the parameter L/l_0 [Fig. 2(a)] and of the parameter $L_z/L_\perp$ [Fig. 2(b)] for $\varepsilon = 0$ and $\alpha = 2$(the first range of the instability). This range of the instability corresponds to the pancake thermal structures of the background turbulent convection ($l_z/l_\perp \approx 2/3$ for $\alpha = 2$). The maximum of the growth rate of the instability ($\gamma_{\max} \approx 0.045\tau_0^{-1}$) reaches at the scale of perturbations $L_m \approx 9.4 l_0$ (for $L_z/L_\perp \approx 0.76$). In this case the threshold of the instability $L_{\rm cr} \approx 4.2 l_0$.

Figure 3 demonstrates the growth rate for the second range of the instability ($\alpha = -3$). Note that this range of the instability corresponds to the thermal structures of the background turbulent convection in the form of columns ($l_z/l_\perp \approx 2$ for $\alpha = -3$). In contrast to the first range of the instability, the growth rate increases with $L_z/L_\perp$ in the whole second range of the instability [see Fig. 3(b)].

B. Mechanism of the convective wind instability

The convective wind instability results in formation of large-scale semiorganized structures in the form of cells (convective wind) in turbulent convection. The mechanism of the convective wind instability, associated with the first term $\mathbf{\Phi} \propto -\tau_0 \alpha (\nabla \cdot \overline{\mathbf{U}}_\perp) \mathbf{\Phi}_\parallel^*$ in the expression for the turbulent flux of entropy [see Eq. (22)], in the shear-free turbulent convection at $\alpha > 0$ is as follows. Perturbations of the vertical velocity $\overline{U}_z$ with $\partial \overline{U}_z/\partial z > 0$ have negative divergence of the horizontal velocity, i.e., $\mathrm{div}\,\overline{\mathbf{U}}_\perp < 0$ (provided that $\mathrm{div}\,\overline{\mathbf{U}} \approx 0$). This results in the vertical turbulent flux of entropy $\tilde{\Phi}_z \propto -\mathrm{div}\,\overline{\mathbf{U}}_\perp$, and it causes an increase of the mean entropy ($\overline{S} \propto \beta^{-1/2} \overline{U}_z \Phi^*/u_0^2$) [see Eqs. (27), (28), and (32)].

On the other hand, the increase of the mean entropy increases the buoyancy force $\propto g\overline{S}$ and results in the increase of the vertical velocity $\overline{U}_z \propto \tau_0 \beta^{1/2} g \overline{S}$ and excitation of the large-scale instability [see Eqs. (25) and (32)]. Similar phenomenon occurs in the regions with $\partial \overline{U}_z/\partial z < 0$ whereby $\mathrm{div}\,\overline{\mathbf{U}}_\perp > 0$. This causes a downward flux of the entropy and

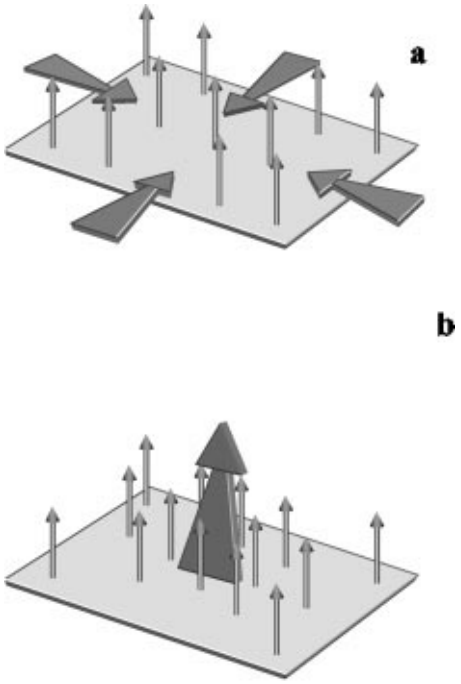

FIG. 4. The effect of a nonzero div $\overline{\mathbf{U}}_\perp$ which causes a redistribution of the vertical turbulent flux of the entropy and results in a formation of a large-scale circulation of the velocity field. Fluid flow with div $\overline{\mathbf{U}}_\perp<0$ (a) produces regions with vertical fluxes of entropy and vertical fluid flow (b) in these regions.

the decrease of the mean entropy. The latter enhances the downward flow and results in the instability which causes formation of a large-scale semiorganized convective wind structure. Thus, nonzero div $\overline{\mathbf{U}}_\perp$ causes redistribution of the vertical turbulent flux of entropy and formation of regions with large vertical fluxes of entropy (see Fig. 4). This results in a formation of a large-scale circulation of the velocity field. This mechanism determines the first range for the instability.

The large-scale circulation of the velocity field causes a nonzero mean vorticity $\overline{\boldsymbol{\omega}}$, and the second term [proportional to $(\alpha+3/2)(\overline{\boldsymbol{\omega}}\times\boldsymbol{\Phi}_\parallel^*)$] in the turbulent flux of entropy (22) is responsible for the formation of a horizontal turbulent flux of the entropy. This causes a decrease of the growth rate of the convective wind instability (for $\alpha>0$), because it decreases the mean entropy $\overline{S}$ in the regions with $\partial\overline{U}_z/\partial z>0$. The net effect is determined by a competition between these effects which are described by the first and second terms in the turbulent flux of entropy (22). The latter determines a lower positive limit $\alpha_{\min}=3/8$ of the parameter α.

When $\alpha<-3/2$ the signs of the first and second terms in expression (22) for the turbulent flux of entropy change. Thus, another mechanism of the convective wind instability is associated with the second term in expression (22) for the turbulent flux of entropy when $\alpha<-3/2$. This term describes the horizontal flux of the mean entropy $\boldsymbol{\Phi}_y\propto\tau_0(\alpha+3/2)(\overline{\boldsymbol{\omega}}\times\boldsymbol{\Phi}_\parallel^*)$. The latter results in the increase (decrease) of the mean entropy in the regions with upward (downward) fluid flows (see Fig. 5). On the other hand, the increase of the

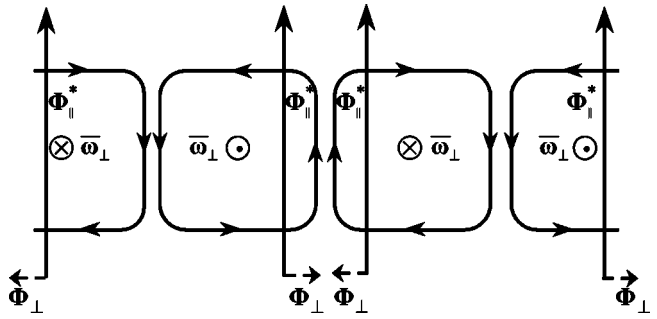

FIG. 5. The effect of a nonzero $\overline{\boldsymbol{\omega}}\times\boldsymbol{\Phi}_\parallel^*$ which induces the horizontal flux of the mean entropy $\boldsymbol{\Phi}_y$ and causes increase (decrease) the mean entropy in the regions with upward (downward) fluid flow when $\alpha<-3/2$.

mean entropy results in the increase of the buoyancy force, the mean vertical velocity $\overline{U}_z$ and the mean vorticity $\overline{\boldsymbol{\omega}}$. The latter amplifies the horizontal turbulent flux of entropy $\boldsymbol{\Phi}_y$ and causes the large-scale convective wind instability. This mechanism determines the second range for the convective wind instability. The first term in the turbulent flux of entropy at $\alpha<0$ causes a decrease of the growth rate of the instability because, when $\alpha<0$, it implies a downward turbulent flux of entropy in the upward flow. This decreases both, the mean entropy and the buoyancy force. Note that, when $\alpha<-3/2$, the thermal structure of the background turbulence has the form of a thermal column or jets: $l_z/l_\perp>3.34$. Even for $\alpha<0$, the ratio $l_z/l_\perp>1.54$.

IV. CONVECTIVE SHEAR INSTABILITY

Let us consider turbulent convection with a linear shear $\overline{\mathbf{U}}^{(0)}=(\lambda/\tau_0)z\mathbf{e}_y$ and a nonzero vertical flux of entropy $\boldsymbol{\Phi}=\Phi_z^{(\mathrm{eq})}\mathbf{e}$, where λ is dimensionless parameter which characterizes the shear. We also consider an isentropic basic reference state, i.e., we neglected a term which is proportional to $(N_b+\partial\overline{S}^{(\mathrm{eq})}/\partial z)\overline{U}_z^{(1)}$ in Eq. (27). We seek for a solution of Eqs. (25)–(27) in the form $\overline{\mathbf{U}}^{(1)}=\overline{\mathbf{V}}\exp(\gamma_{\mathrm{inst}}t)\cos(\Omega t+\mathbf{K}\cdot\mathbf{R})$. Here, for simplicity, we study the case $K_y=\mathbf{0}$.

A. The growth rate of convective shear instability

Using a procedure similar to that employed for the analysis of the convective wind instability we found that the growth rate of the convective shear instability is determined by a cubic equation

$$(\tilde{\gamma}+B_3)(\tilde{\gamma}^2+A\tilde{\gamma}-B)+8\beta^2\gamma_0^3=0, \tag{35}$$

where $\tilde{\gamma}=(\gamma_{\mathrm{inst}}+i\Omega)/\nu_T K^2$, $\gamma_0=(1/2)c_9^{1/3}(\lambda X)^{2/3}$, $c_9=18\mu b_*/5$, $b_*=-\Phi_y^{(\mathrm{eq})}(1+\varepsilon/2)/(\lambda\Phi_z^{(\mathrm{eq})})$, and $B_3=c_1+c_2X$, $c_2=\varepsilon(q+1)/4$. The growth rate of the instability for $\beta\gg1$ is given by

$$\gamma_{\mathrm{inst}}\simeq\nu_T K^2\left(\beta^{2/3}\gamma_0+\beta^{1/3}\frac{C}{12\gamma_0}\right), \tag{36}$$

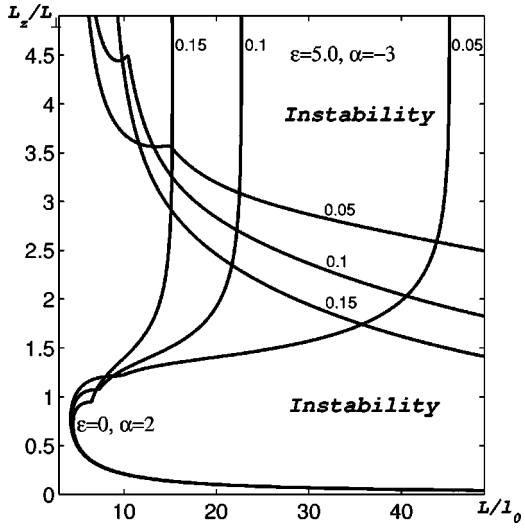

FIG. 6. The range of parameters $(L_z/L_\perp; L/l_0)$ for which the convective shear instability occurs, for $\alpha=2$, $\varepsilon=0$, and $\alpha=-3$, $\varepsilon=5$ for different values of the shear $\lambda=0.05;0.1;0.15$.

where $C=X(c_7-c_8X)$. The instability results in the generation of the convective shear waves with the frequency

$$\Omega \simeq \sqrt{3}\,\nu_T K^2\left(\beta^{2/3}\gamma_0-\beta^{1/3}\frac{C}{12\gamma_0}\right). \tag{37}$$

The flow in the convective shear wave has a nonzero hydrodynamic helicity

$$\chi \equiv \overline{\mathbf{V}}\cdot(\boldsymbol{\nabla}\times\overline{\mathbf{V}}) = -\frac{2\lambda\Omega K_x\overline{\mathbf{V}}^2}{\tau_0(\Omega^2+\gamma_{\rm inst}^2)}. \tag{38}$$

Therefore, for $\lambda>0$ the mode with $K_x>0$ has a negative helicity and the mode with $K_x<0$ has a positive helicity.

Figure 6 shows the range of parameters $L_z/L_\perp$ and L/l_0 where the convective shear instability occurs, for $\alpha=2$, $\varepsilon=0$ and for different values of the shear $\lambda=0.05;0.1;0.15$. There are two ranges for the instability. However, even a small shear causes an overlapping of the two ranges for the instability and the increase of shear (λ) promotes the convective shear instability.

Figures 7 and 8 demonstrate the growth rates of the convective shear instability and the frequencies of the generated convective shear waves for the first $(\alpha=2)$ and second $(\alpha=-3)$ ranges of the instability. The curves in Figs. 6–8 have a point L_* whereby the first derivative $d\gamma_{\rm inst}/dK$ has a singularity. At this point there is a bifurcation which is illustrated in Figs. 7 and 8. The growth rate of the convective shear instability is determined by cubic algebraic equation (35). Before the bifurcation point $(L<L_*)$, the cubic equation has three real roots (which corresponds to aperiodic instability). After the bifurcation point $(L>L_*)$, the cubic equation has one real and two complex conjugate roots. When $L>L_*$ the convective shear waves are generated. When the parameter $L_z/L_\perp$ increases, the value L_* decreases. When $L_z>L_\perp$, the bifurcation point $L_*<L_{\rm cr}$. For a given parameter L/l_0 there are the lower and upper bounds

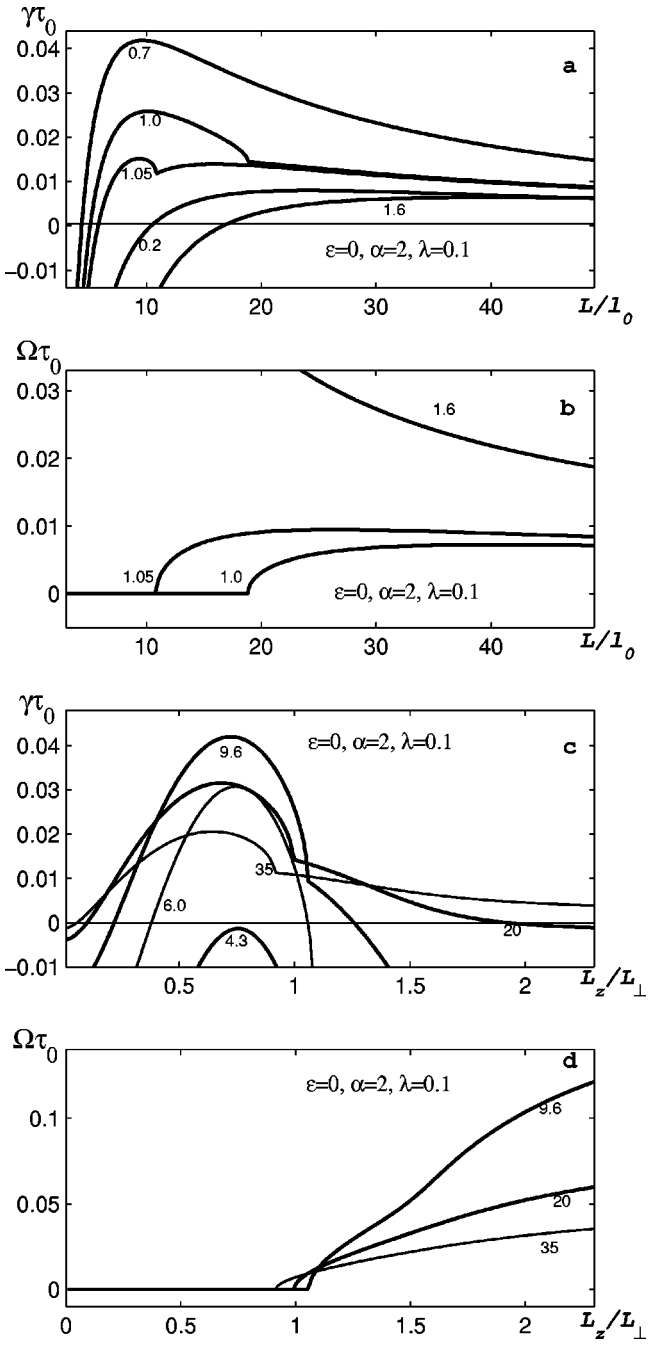

FIG. 7. The growth rates of the convective shear instability (a) and (c) and the frequencies of the generated convective shear waves (b) and (d) for the first $(\alpha=2)$ range of the instability and for $\varepsilon=0$. Corresponding dependencies on the parameter L/l_0 are given for different $L_z/L_\perp$ and vice versa.

for the parameter $L_z/L_\perp$ when the convective shear instability occurs. For large enough parameter $L=L_u$ the upper limit of the range of the instability does not exist, e.g., for $\lambda=0.05$ the parameter $L_u=47l_0$ and for $\lambda=0.15$ the parameter $L_u=13l_0$.

Note that when $L<L_*$ the convective shear waves are not generated and the properties of the convective shear instability are similar to that of the convective wind instability [compare Fig. 2(b) and the curve for $L/l_0=6$ in Fig. 8(c)].

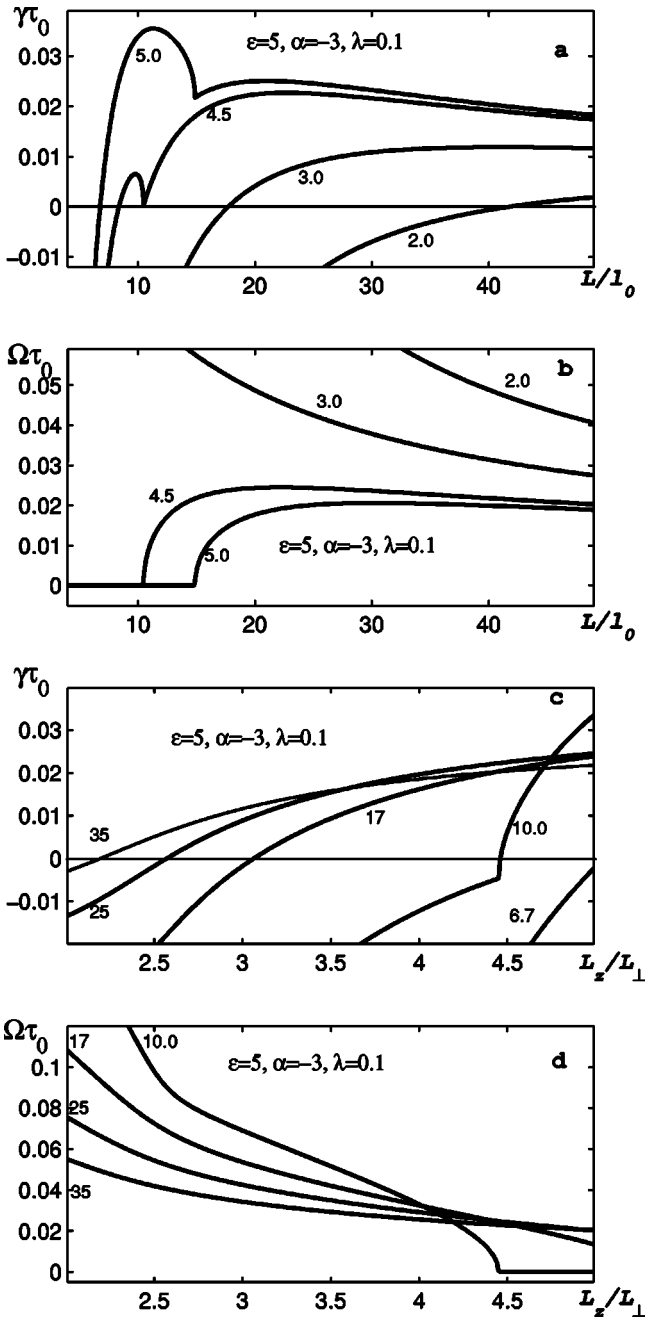

FIG. 8. The growth rates of the convective shear instability (a) and (c) and the frequencies of the generated convective shear waves (b) and (d) for the second ($\alpha=-3$) range of the instability and for $\varepsilon=0$. Corresponding dependencies on the parameter L/l_0 are given for different $L_z/L_\perp$ and vice versa.

However, for $L>L_*$ these two instabilities are totally different. The properties of the convective shear instability in the first and in the second ranges of the instability are different. In particular, in the second range of the convective shear instability the growth rate monotonically increases, and the frequency of the generated convective shear waves decreases with the parameter $L_z/L_\perp$.

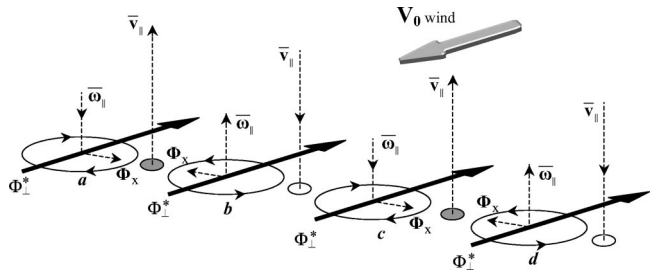

FIG. 9. The effect of a nonzero $\overline{\boldsymbol{\omega}}_\parallel\times\boldsymbol{\Phi}^*$ which causes a redistribution of the horizontal turbulent flux of the entropy. For two vortices (a and b) with opposite directions of the vorticity $\overline{\boldsymbol{\omega}}_\parallel$, the turbulent flux of entropy is directed towards the boundary between the vortices. The latter increases the mean entropy between the vortices (a and b). Similarly, the mean entropy between the vorticies b and c decreases.

B. Mechanism of convective shear instability

The mechanism of the convective shear instability associated with the last term in expression (22) for the turbulent flux of entropy [$\boldsymbol{\Phi}\propto\tau_0(\overline{\boldsymbol{\omega}}_\parallel\times\boldsymbol{\Phi}^*)$] is as follows. The vorticity perturbations $\overline{\omega}\equiv(\boldsymbol{\nabla}\times\overline{\mathbf{U}})_z$ generate perturbations of entropy: $\overline{S}\propto\beta^{-1/6}(\tau_0/u_0)\Phi_y^*\lambda^{-2/3}\exp(i\pi/6)\overline{\omega}$. Indeed, consider two vortices (say, ''a'' and ''b'' in Fig. 9) with the opposite directions of the vorticity $\overline{\boldsymbol{\omega}}_\parallel$. The turbulent flux of entropy is directed towards the boundary between the vortices. The latter increases the mean entropy between the vortices (a and b).

Similarly, the mean entropy between the vorticies ''b'' and ''c'' decreases (see Fig. 9). Such redistribution of the mean entropy causes increase (decrease) of the buoyancy force and formation of upward (downward) flows between the vortices a and b (b and c): $\overline{U_z}\propto\beta^{1/3}\lambda^{-2/3}g\tau_0\exp(-i\pi/3)\overline{S}$. Finally, the vertical flows generate vorticity $\overline{\omega}\propto-\beta^{-1/6}\lambda^{1/3}\exp(i\pi/6)\overline{U_z}/l_0$, etc. This results in the excitation of the instability with the growth rate $\gamma_{\rm inst}\propto K^{2/3}$ and the generation of the convective shear waves with the frequency $\Omega\propto K^{2/3}$. For perturbations with $K_x=0$ the convective shear instability does not occur. However, for these perturbations with $K_x=0$ the convective wind instability can be excited (see Sec. III), and it is not accompanied by the generation of the convective shear waves. We considered here a linear shear for simplicity. The equilibrium is also possible for a quadratic shear, i.e., when $\overline{\mathbf{U}}^{(0)}=\tilde{\lambda}z^2\mathbf{e}_y$.

V. DISCUSSION

The convective wind theory of turbulent sheared convection is proposed. The developed theory predicts the convective wind instability in a shear-free turbulent convection. This instability causes the formation of large-scale semiorganized fluid motions (convective wind) in the form of cells. Spatial characteristics of these motions, such as the minimum size of the growing perturbations and the size of perturbations with the maximum growth rate, are determined.

This study predicts also the existence of the convective shear instability in the sheared turbulent convection. This instability causes the formation of large-scale semiorganized fluid motions in the form of rolls (sometimes visualized as the boundary layer cloud streets). These motions can exist in the form of generated convective shear waves, which have a nonzero hydrodynamic helicity. Increase of shear promotes excitation of the convective shear instability.

Here the proposed theory of turbulent sheared convection distinguishes between the true turbulence, corresponding to the small-scale part of the spectrum, and the convective wind comprising of large-scale semiorganized motions caused by the inverse energy cascade through large-scale instabilities. The true turbulence in its turn consists of the two parts: the familiar ''Kolmogorov-cascade turbulence'' and an essentially anisotropic tangling turbulence caused by the tangling of the mean-velocity gradients with the Kolmogorov-type turbulence. These two types of turbulent motions overlap in the maximum-scale part of the spectrum. The tangling turbulence does not exhibit any direct energy cascade.

It was demonstrated here that the characteristic length and time scales of the convective wind motions are much larger than the true-turbulence scales. This justifies the separation of scales which is required for the existence of these two types of motions. It is proposed that the term turbulence (or true turbulence) be kept only for the Kolmogorov and tangling turbulence part of the spectrum. This concept implies that the convective wind (as well as semiorganized motions in other very high Reynolds number flows) should not be confused with the true turbulence. The diagram of interactions between turbulent and mean-flow objects which cause the large-scale instability and formation of semiorganized structures is shown in Fig. 10.

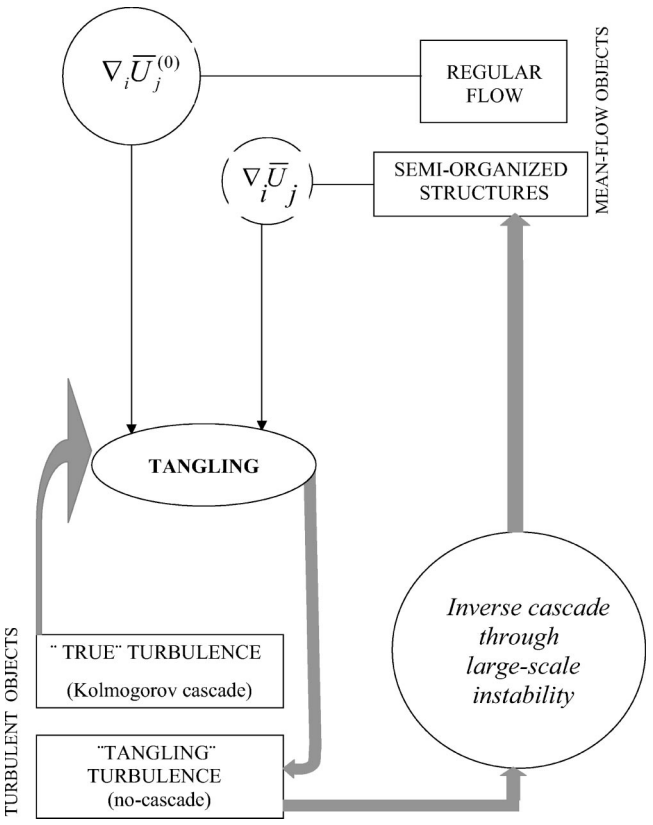

FIG. 10. Scheme of interactions between turbulent and mean-flow objects which cause a large-scale instability.

Now let us compare the obtained results with the properties of semiorganized structures observed in the atmospheric convective boundary layer. The semiorganized structures are observed in the form of rolls (cloud streets) or three-dimensional convective cells (cloud cells). Rolls usually align along or at angles of up to 10° with the mean horizontal wind of the convective layer, with lengths from 20 to 200 km, widths from 2 to 10 km, and convective depths from 2 to 3 km [2]. The typical value of the aspect ratio $L_z/L_\perp \approx 0.14-1$. The ratio of the minimal size of structures to the maximum scale of turbulent motions is $L/l_0 = 10-100$. The characteristic life time of rolls varies from 1 to 72 h [1]. Rolls may occur over both, water surface and land surfaces. The suggested theory predicts the following parameters of the convective rolls: the aspect ratio $L_z/L_\perp$ ranges from very small to 1, and $L/l_0 = 10-100$. The characteristic time of formation of the rolls $\sim \tau_0/\gamma_{\rm inst}$ varies from 1 to 3 h. The life time of the convective rolls is determined by a nonlinear evolution of the convective shear instability. The latter is a subject of a separate ongoing study.

Convective cells may be divided into two types: open and closed. Open-cell circulation has downward motion and clear sky in the cell center, surrounded by cloud associated with upward motion. Closed cells have the opposite circulation [2]. Both types of cells have diameters ranging from 10 to 40 km and aspect ratios $L_z/L_\perp \approx 0.05-1$, and both occur in a convective boundary layer with a depth of about 1 to 3 km. The ratio of the minimum size of structures to the maximum scale of turbulent motions is $L/l_0 = 5-20$. The developed theory predicts the following parameters of the convective cells: the aspect ratio $L_z/L_\perp$ ranges from very small to 1, and $L/l_0 = 5-15$. The characteristic time of formation of the convective cells $\sim \tau_0/\gamma_{\rm inst}$ varies from 1 to 3 h. Therefore the predictions of the developed theory are in a good agreement with observations of the semiorganized structures in the atmospheric convective boundary layer. Moreover, the typical temporal and spatial scales of structures are always much larger than the turbulence scales. This justifies the separation of scales which was assumed in the suggested theory.

ACKNOWLEDGMENTS

We have benefited from valuable suggestions made by Arkady Tsinober. The authors acknowledge useful discussions with Erland Källen and Branko Grisogono at a seminar at the Meteorological Institute of Stockholm University. This work was partially supported by The German-Israeli Project Cooperation (DIP) administrated by the Federal Ministry of Education and Research (BMBF), by the INTAS Program Foundation (Grants No. 00-0309 and 99-348), by the SIDA, Project No. SRP-2000-036, and by the Swedish Institute, Project No. 2570/2002 (381/N34).

APPENDIX A: DERIVATIONS OF EXPRESSIONS FOR THE REYNOLDS STRESSES AND TURBULENT FLUX OF ENTROPY

Equations (2) and (3) yield the following conservation equations for the kinetic energy $W_v=\rho_0\mathbf{v}^2/2$, for $W_S=\rho_0 S^2/2$ and for $\mathbf{W}^\Phi=\rho_0 S\mathbf{v}$:

$$\frac{\partial W_v}{\partial t}+\boldsymbol{\nabla}\cdot\mathbf{F}_v=I_v-D_v, \tag{A1}$$

$$\frac{\partial W_S}{\partial t}+\boldsymbol{\nabla}\cdot\mathbf{F}_S=I_S-D_S, \tag{A2}$$

$$\frac{\partial W_i^\Phi}{\partial t}+\boldsymbol{\nabla}_j\mathbf{F}_{ij}^\Phi=I_i^\Phi-D_i^\Phi, \tag{A3}$$

where $I_v=-\rho_0(\mathbf{v}\cdot\mathbf{g})S$, $I_S=-I_v\Omega_b^2/g^2$, and $\mathbf{I}^\Phi=-\rho_0[\mathbf{v}(\mathbf{v}\cdot\mathbf{N}_b)+S^2\mathbf{g}]+(P/\rho_0)\boldsymbol{\nabla}(S\rho_0)$ are the source terms in these equations, $D_v=-\rho_0(\mathbf{v}\cdot\mathbf{f}_\nu)$, $D_S=\rho_0 S(\boldsymbol{\nabla}\cdot\mathbf{F}_\kappa)$, and $\mathbf{D}^\Phi=-\rho_0 S\mathbf{f}_\nu+(\rho_0/T_0)\mathbf{v}(\boldsymbol{\nabla}\cdot\mathbf{F}_\kappa)$ are the dissipative terms, $\mathbf{F}_v=\mathbf{v}(W_v+P)$, $\mathbf{F}_S=\mathbf{v}W_S$, and $\mathbf{F}_{ij}^\Phi=\rho_0 S v_i v_j+SP\delta_{ij}$ are the fluxes. Equations (A1) and (A2) yield conservation equation for $W_E=W_v\Omega_b^2/g^2+W_S$,

$$\frac{\partial W_E}{\partial t}+\boldsymbol{\nabla}\cdot\mathbf{F}_E=-D_E, \tag{A4}$$

where $D_E=D_v\Omega_b^2/g^2+D_S$ is the dissipative term and $\mathbf{F}_E=\mathbf{F}_v\Omega_b^2/g^2+\mathbf{F}_S$ is the flux. Equation (A4) does not have a source term, and this implies that without dissipation ($D_E=0$) the value $\int W_E dV$ is conserved, where in the latter formula the integration is performed over the volume. For the convection $\Omega_b^2<0$ and, therefore, $W_S\approx W_v|\Omega_b^2|/g^2$.

Using Eqs. (A1)–(A3) we derived balance equations for the second moments. In particular, averaging Eqs. (A1)–(A3) over the ensemble of fluctuations and subtracting from these equations the corresponding equations for the mean fields: $\rho_0\overline{\mathbf{U}}^2/2$, $\rho_0\overline{S}^2/2$, $\rho_0\overline{S}\overline{\mathbf{U}}$, yields

$$\left(\frac{\partial}{\partial t}+\overline{\mathbf{U}}\cdot\boldsymbol{\nabla}\right)f_{pp}+2f_{ij}\nabla_j\overline{U}_i+2\boldsymbol{\Phi}\cdot\mathbf{g}+\frac{2}{\rho_0}\boldsymbol{\nabla}\cdot\boldsymbol{\Psi}_E=-\frac{f_*}{\tau_0\delta_*}\left(1+\frac{\varepsilon}{2}\right), \tag{A5}$$

$$\left(\frac{\partial}{\partial t}+\overline{\mathbf{U}}\cdot\boldsymbol{\nabla}\right)\Phi_i+(\boldsymbol{\Phi}\cdot\boldsymbol{\nabla})\overline{U}_i+f_{ij}(\mathbf{N}_b+\boldsymbol{\nabla}\overline{S})_j-\frac{1}{2}ge_i(4-\gamma)H+\frac{1}{\rho_0}\nabla_j\Psi_{ij}-\left(\frac{\gamma P_0}{\rho_0}\right)H(\mathbf{N}_b)_i=-\frac{\Phi_i^*}{2\tau_0\delta_*}(1+\mathrm{Pr}), \tag{A6}$$

$$\left(\frac{\partial}{\partial t}+\overline{\mathbf{U}}\cdot\boldsymbol{\nabla}\right)H+2\Phi_j(\mathbf{N}_b+\boldsymbol{\nabla}\overline{S})_j=-\frac{H_*}{\tau_0\delta_*}, \tag{A7}$$

where $\mathrm{Pr}=\nu/\kappa$ is the Prandtl number, ν is the kinematic viscosity, $\boldsymbol{\Psi}_E=\rho_0 f_{pp}\mathbf{u}/2+\langle p\mathbf{u}\rangle$, $\Psi_{ij}=\rho_0\langle s u_i u_j\rangle+\delta_{ij}(\gamma P_0 H/2+\langle sp\rangle)$, and we took into account that the dissipations of energy, the flux of entropy and the second moment of entropy H are determined by the background turbulent convection described by Eqs. (12)–(17). In derivation of Eq. (A6) we used an identity $\rho_0 S\boldsymbol{\nabla}(P/\rho_0)\simeq\boldsymbol{\nabla}(\gamma P_0 S^2)/2+\gamma P_0 S^2\mathbf{N_b}+(\gamma/2-1)\rho_0\mathbf{g}S^2$, and we assumed that $S\simeq P/\gamma P_0$, i.e., we neglected fluctuations of density ρ/ρ_0. Equations (A5)–(A7) allow us to determine f_*, $\boldsymbol{\Phi}^*$, and H_* in the background turbulent convection (see below).

Using Eqs. (6) and (7) we derived equations for the following second moments:

$$f_{ij}(\mathbf{k},\mathbf{R})=\langle u_i(\mathbf{k},\mathbf{R})u_j(-\mathbf{k},\mathbf{R})\rangle, \tag{A8}$$

$$\Phi_i(\mathbf{k},\mathbf{R})=\langle s(\mathbf{k},\mathbf{R})u_i(-\mathbf{k},\mathbf{R})\rangle, \tag{A9}$$

$$F(\mathbf{k},\mathbf{R})=\langle s(\mathbf{k},\mathbf{R})\omega(-\mathbf{k},\mathbf{R})\rangle, \tag{A10}$$

$$G(\mathbf{k},\mathbf{R})=\langle \omega(\mathbf{k},\mathbf{R})\omega(-\mathbf{k},\mathbf{R})\rangle, \tag{A11}$$

$$H(\mathbf{k},\mathbf{R})=\langle s(\mathbf{k},\mathbf{R})s(-\mathbf{k},\mathbf{R})\rangle, \tag{A12}$$

where $\omega\equiv(\boldsymbol{\nabla}\times\mathbf{u})_z$ and we use a two-scale approach, i.e., a correlation function is written as follows:

$$\langle u_i(\mathbf{x})u_j(\mathbf{y})\rangle=\int\langle u_i(\mathbf{k}_1)u_j(\mathbf{k}_2)\rangle\exp[i(\mathbf{k}_1\cdot\mathbf{x}+\mathbf{k}_2\cdot\mathbf{y})]\times d\mathbf{k}_1 d\mathbf{k}_2=\int f_{ij}(\mathbf{k},\mathbf{R})\exp(i\mathbf{k}\cdot\mathbf{r})d\mathbf{k},$$

$$f_{ij}(\mathbf{k},\mathbf{R})=\int\langle u_i(\mathbf{k}+\mathbf{K}/2)u_j(-\mathbf{k}+\mathbf{K}/2)\rangle\exp(i\mathbf{K}\cdot\mathbf{R})d\mathbf{K}$$

(see, e.g., [37,38]), where $\mathbf{R}$ and $\mathbf{K}$ correspond to the large scales, and $\mathbf{r}$ and $\mathbf{k}$ to the small scales, i.e., $\mathbf{R}=(\mathbf{x}+\mathbf{y})/2$, $\mathbf{r}=\mathbf{x}-\mathbf{y}$, $\mathbf{K}=\mathbf{k}_1+\mathbf{k}_2$, $\mathbf{k}=(\mathbf{k}_1-\mathbf{k}_2)/2$. This implies that we assumed that there exists a separation of scales, i.e., the maximum scale of turbulent motions l_0 is much smaller than the characteristic scale L of inhomogeneities of the mean fields. In particular, this implies that $r\leqslant l_0\ll R$. Our final results showed that this assumption is indeed valid. Now let us calculate

$$\frac{\partial f_{ij}(\mathbf{k}_1,\mathbf{k}_2)}{\partial t}\equiv\left\langle P_{in}(\mathbf{k}_1)\frac{\partial u_n(\mathbf{k}_1)}{\partial t}u_j(\mathbf{k}_2)\right\rangle+\left\langle u_i(\mathbf{k}_1)P_{jn}(\mathbf{k}_2)\frac{\partial u_n(\mathbf{k}_2)}{\partial t}\right\rangle, \tag{A13}$$

$$\frac{\partial\Phi_j(\mathbf{k}_1,\mathbf{k}_2)}{\partial t}\equiv\left\langle s(\mathbf{k}_1)P_{jn}(\mathbf{k}_2)\frac{\partial u_n(\mathbf{k}_2)}{\partial t}\right\rangle+\left\langle\frac{\partial s(\mathbf{k}_1)}{\partial t}u_j(\mathbf{k}_2)\right\rangle, \tag{A14}$$

where we multiplied equation of motion (6) rewritten in $\mathbf{k}$ space by $P_{ij}(\mathbf{k})=\delta_{ij}-k_{ij}$ in order to exclude the pressure term from the equation of motion.

Thus, equations for $f_{ij}(\mathbf{k},\mathbf{R})$ and $\boldsymbol{\Phi}(\mathbf{k},\mathbf{R})$ read

$$\frac{\partial f_{ij}(\mathbf{k})}{\partial t} = \hat{I}_{ijmn} f_{mn}(\mathbf{k}) + N_{ij}(\mathbf{k}), \tag{A15}$$

$$\frac{\partial \Phi_i(\mathbf{k})}{\partial t} = \hat{I}_{ij} \Phi_j(\mathbf{k}) + M_i(\mathbf{k}), \tag{A16}$$

where

$$\hat{I}_{ijmn} = 2(k_{iq}\delta_{mp}\delta_{jn} + k_{jq}\delta_{im}\delta_{pn})\nabla_p \overline{U}_q - \left(\delta_{im}\delta_{jq}\delta_{np} + \delta_{iq}\delta_{jn}\delta_{mp} - \delta_{im}\delta_{jn}k_q \frac{\partial}{\partial k_p} \right) \nabla_p \overline{U}_q, \tag{A17}$$

$$\hat{I}_{ij} = 2k_{in}\nabla_j \overline{U}_n + \delta_{ij}k_n \frac{\partial}{\partial k_m}\nabla_m \overline{U}_n - \nabla_j \overline{U}_i, \tag{A18}$$

$$N_{ij}(\mathbf{k}) = g e_m [P_{im}(\mathbf{k})\Phi_j(\mathbf{k}) + P_{jm}(\mathbf{k})\Phi_i(-\mathbf{k})] + f_{ij}^N(\mathbf{k}), \tag{A19}$$

$$M_i(\mathbf{k}) = -f_{mi}(\mathbf{N}_b + \boldsymbol{\nabla}\overline{S})_m + g e_m P_{im}(\mathbf{k}) H + \Phi_i^N, \tag{A20}$$

and hereafter we consider the case with $\boldsymbol{\nabla}\cdot\overline{\mathbf{U}}=0$ (i.e., $\Lambda=0$). Here f_{ij}^N and Φ_i^N are the third moments appearing due to the nonlinear terms. Equations (A15) and (A16) are written in a frame moving with a local velocity $\overline{\mathbf{U}}$ of the mean flow. In Eqs. (A15)–(A20) we neglected small terms which are of the order of $O(\nabla^3\overline{\mathbf{U}})$ and $O(\nabla^2 f_{ij}; \nabla^2\Phi_i)$. Note that Eqs. (A15)–(A20) do not contain the terms proportional to $O(\nabla^2\overline{\mathbf{U}})$. The first term in the right hand side of Eqs. (A15) and (A16) depends on the gradients of the mean fluid velocity ($\nabla_i \overline{U}_j$). Equations for the second moments $G(\mathbf{k})$, $F(\mathbf{k})$, and $H(\mathbf{k})$ read

$$\frac{\partial G(\mathbf{k})}{\partial t} = (\mathbf{e}\times\tilde{\mathbf{k}}_1)_i (\mathbf{e}\times\tilde{\mathbf{k}}_2)_j \frac{\partial f_{ij}(\mathbf{k})}{\partial t}, \tag{A21}$$

$$\frac{\partial F(\mathbf{k})}{\partial t} = -i(\mathbf{e}\times\tilde{\mathbf{k}}_1)_j \frac{\partial \Phi_j(\mathbf{k})}{\partial t}, \tag{A22}$$

$$\frac{\partial H(\mathbf{k})}{\partial t} = Q(\mathbf{k}), \tag{A23}$$

where $Q(\mathbf{k}) = -2\boldsymbol{\Phi}(\mathbf{k})\cdot(\mathbf{N}_b + \boldsymbol{\nabla}\overline{S}) + H_N$, and H_N is the third moment appearing due to the nonlinear terms, $\tilde{\mathbf{k}}_1 = \mathbf{k} - (i/2)\boldsymbol{\nabla}$, $\tilde{\mathbf{k}}_2 = \mathbf{k} + (i/2)\boldsymbol{\nabla}$. The terms $\sim\boldsymbol{\Phi}$ in the tensor $N_{ij}(\mathbf{k})$ [see Eqs. (A15) and (A19)] can be considered as a stirring force for the turbulent convection. On the other hand, the terms $\sim(\mathbf{N}_b + \boldsymbol{\nabla}\overline{S})$ in Eqs. (A16), (A20), and (A23) are the sources of the flux of entropy $\boldsymbol{\Phi}$ and the second moment of entropy H. Note that a stirring force in the Navier-Stokes turbulence is an external parameter.

Since the equations for the second moments contain the third moments, a problem of closure for the higher moments arises. In this study we used the τ approximation [see Eq. (11)] which allows us to express the third moments f_{ij}^N, $\boldsymbol{\Phi}^N$, and H_N in Eqs. (A15), (A16), and (A23) in terms of the second moments. Here we define a background turbulent convection as the turbulent convection with zero gradients of the mean fluid velocity ($\nabla_i \overline{U}_j = 0$)]. The background turbulent convection is determined by the following equations:

$$\frac{\partial f_{ij}^{(0)}(\mathbf{k})}{\partial t} = N_{ij}^{(0)}(\mathbf{k}), \tag{A24}$$

$$\frac{\partial \Phi_i^{(0)}(\mathbf{k})}{\partial t} = M_i^{(0)}(\mathbf{k}), \tag{A25}$$

$$\frac{\partial H^{(0)}(\mathbf{k})}{\partial t} = Q^{(0)}(\mathbf{k}). \tag{A26}$$

A nonzero gradient of the mean fluid velocity results in deviations from the background turbulent convection. These deviations are determined by the following equations:

$$\frac{\partial (f_{ij} - f_{ij}^{(0)})}{\partial t} = \hat{I}_{ijmn} f_{mn}(\mathbf{k}) - \frac{f_{ij} - f_{ij}^{(0)}}{\tau(k)}, \tag{A27}$$

$$\frac{\partial (\Phi_i - \Phi_i^{(0)})}{\partial t} = \hat{I}_{ij}\Phi_j(\mathbf{k}) - \frac{\Phi_i - \Phi_i^{(0)}}{\tau(k)}, \tag{A28}$$

$$\frac{\partial (H - H^{(0)})}{\partial t} = -\frac{H - H^{(0)}}{\tau(k)}, \tag{A29}$$

where the deviations (caused by a nonzero gradients of the mean fluid velocity) of the functions $N_{ij}(\mathbf{k}) - N_{ij}^{(0)}(\mathbf{k})$ and $M_i(\mathbf{k}) - M_i^{(0)}(\mathbf{k})$ from the background state are described by the relaxation terms: $-(f_{ij} - f_{ij}^{(0)})/\tau(k)$ and $-(\Phi_i - \Phi_i^{(0)})/\tau(k)$, respectively. Similarly, the deviation $Q(\mathbf{k}) - Q^{(0)}(\mathbf{k})$ is described by the term $-(H - H^{(0)})/\tau(k)$. Here we assumed that the correlation time $\tau(k)$ is independent of the gradients of the mean fluid velocity.

Now we assume that the characteristic times of variation of the second moments $f_{ij}(\mathbf{k})$, $\Phi_i(\mathbf{k})$, and $H(\mathbf{k})$ are substantially larger than the correlation time $\tau(k)$ for all turbulence scales. This allows us to determine a stationary solution for the second moments $f_{ij}(\mathbf{k})$, $\Phi_i(\mathbf{k})$, and $H(\mathbf{k})$,

$$f_{ij}(\mathbf{k}) = f_{ij}^{(0)}(\mathbf{k}) + \tau(k)\hat{I}_{ijmn} f_{mn}^{(0)}(\mathbf{k}), \tag{A30}$$

$$\Phi_i(\mathbf{k}) = \Phi_i^{(0)}(\mathbf{k}) + \tau(k)\hat{I}_{ij}\Phi_j^{(0)}(\mathbf{k}), \tag{A31}$$

$$H(\mathbf{k}) = H^{(0)}(\mathbf{k}), \tag{A32}$$

where we neglected the third and higher-order spatial derivatives of the mean-velocity field $\overline{\mathbf{U}}$.

For the integration in $\mathbf{k}$ space of the second moments $f_{ij}(\mathbf{k})$, $\Phi_i(\mathbf{k})$, ..., $H(\mathbf{k},\mathbf{R})$ we have to specify a model for the background turbulent convection. We used the model of the background turbulent convection determined by Eqs. (12)–(17). For the integration in $\mathbf{k}$ space we used identities given in Appendix C. The integration in $\mathbf{k}$ space of Eqs.

(A30) and (A31) yields the following equations for the Reynolds stresses and the turbulent flux of entropy:

$$f_{ij}=f_{ij}^{(0)}-\nu_T\Bigg(a_1(\nabla_i\overline{U}_j+\nabla_j\overline{U}_i)+a_2(e_i\nabla_j+e_j\nabla_i)\overline{U}_z - c_2\frac{\partial}{\partial z}(e_i\overline{U}_j+e_j\overline{U}_i)+\frac{\partial\overline{U}_z}{\partial z}(c_3e_{ij}+a_3\delta_{ij})\Bigg), \tag{A33}$$

$$\mathbf{\Phi}=\mathbf{\Phi}^*+\frac{\tau_0}{30}(\mathbf{\Phi}^*\cdot\mathbf{e})\Bigg(\frac{\partial}{\partial z}(b_1\overline{U}_z\mathbf{e}+b_2\overline{\mathbf{U}})-b_3\nabla^\perp\overline{U}_z\Bigg) - \frac{\tau_0}{5}\{2(\mathbf{\Phi}^*\times\mathbf{e})\overline{\omega}+5(\mathbf{\Phi}^*\cdot\nabla)\overline{\mathbf{U}}-2(\mathbf{\Phi}^*\cdot\nabla_\perp) \times\overline{\mathbf{U}}+(3-q)(\mathbf{e}\times\nabla)[\mathbf{\Phi}^*\cdot(\mathbf{e}\times\overline{\mathbf{U}})]-(q-1)[(\mathbf{\Phi}^* \times\mathbf{e})\cdot\nabla](\mathbf{e}\times\overline{\mathbf{U}})\}, \tag{A34}$$

where $\nu_T=\tau_0 f_*/6$, $\overline{\omega}=(\nabla\times\overline{\mathbf{U}})_z$, $a_1=c_1+c_2$, $a_2=-\varepsilon(q-1)/4$, $a_3=-\varepsilon(5-q)/4$, $b_1=(8\alpha-3)(q+1)$, $b_2=3(9-q)-2\alpha(q+1)$, $b_3=(2\alpha+3)(q+1)$, $c_1=(q+3)/5$, $c_2=\varepsilon(q+1)/4$, $c_3=\varepsilon(q+3)/4$.

Equations (A33) and (A34) imply that there are two contributions to the Reynolds stresses and turbulent flux of entropy which correspond to two kinds of fluctuations of the velocity field. The first contribution is due to the Kolmogorov turbulence with the spectrum ($\propto k^{-q}$), and it corresponds to the background turbulent convection. The second kind of fluctuations depends on gradients of the mean-velocity field and is caused by a tangling of gradients of the mean-velocity field by turbulent motions. The spectrum of the tangling turbulence is $W(k)\tau(k)\propto k^{1-2q}$ [see Eqs. (A30) and (A31)]. These fluctuations describe deviations from the background turbulent convection caused by the gradients of the mean fluid velocity field.

Now we calculate a dissipation of the kinetic energy of the mean flow $\overline{\mathbf{U}}$,

$$D_U\equiv-(1/2)(f_{ij}-f_{ij}^{(0)})(\nabla_i\overline{U}_j+\nabla_j\overline{U}_i), \tag{A35}$$

using a general form of the velocity field $\overline{U}_i=\overline{V}_i(t,\mathbf{K})\exp(i\mathbf{K}\cdot\mathbf{R})$, where

$$\overline{V}_i(t,\mathbf{K})=\left(\frac{K}{K_\perp}\right)^2[P_{ij}(\mathbf{K})e_j\overline{V}_z(t,\mathbf{K})-iK^{-2}(\mathbf{e}\times\mathbf{K})_i\widetilde{\omega}(t,\mathbf{K})], \tag{A36}$$

and $\widetilde{\omega}=(\nabla\times\overline{\mathbf{V}})_z$. The result is given by

$$D_U(t,\mathbf{K})=\nu_T\Bigg\{b_4\left(\frac{K}{K_\perp}\right)^2[K^2\overline{V}_z^2(t,\mathbf{K})+\widetilde{\omega}^2(t,\mathbf{K})] +b_5K^2\overline{V}_z^2(t,\mathbf{K})\Bigg\}, \tag{A37}$$

where $b_4=c_1+c_2\sin^2\theta$ and $b_5=a_2+c_3\cos^2\theta$. The function $D_U(t,\mathbf{K})$ must be positive for statistically stationary small-scale turbulence. The latter is valid when ε satisfies condition (21).

APPENDIX B: THE MODEL OF THE BACKGROUND TURBULENT CONVECTION

A simple approximate model for the three-dimensional isotropic Navier-Stokes turbulence is described by a two-point correlation function of the velocity field $f_{ij}(t,\mathbf{x},\mathbf{y})=\langle u_i(t,\mathbf{x})u_j(t,\mathbf{y})\rangle$ with the Kolmogorov spectrum $W(k)\propto k^{-q}$ and $q=5/3$. The turbulent convection is determined not only by the turbulent velocity field $\mathbf{u}(t,\mathbf{x})$, but by the fluctuations of the entropy $s(t,\mathbf{x})$. This implies that for the description of the turbulent convection one needs additional correlation functions, e.g., the turbulent flux of entropy $\mathbf{\Phi}_i(t,\mathbf{x},\mathbf{y})=\langle s(t,\mathbf{x})u_i(t,\mathbf{y})\rangle$ and the second moment of the entropy fluctuations $H(t,\mathbf{x},\mathbf{y})=\langle s(t,\mathbf{x})s(t,\mathbf{y})\rangle$. Note also that the turbulent convection is anisotropic.

Let us derive Eqs. (12) and (13) for the correlation functions f_{ij} and $\mathbf{\Phi}_i$. To this end, the velocity $\mathbf{u}_\perp$ is written as a sum of the vortical and the potential components, i.e., $\mathbf{u}_\perp=\nabla\times(\widetilde{C}\mathbf{e})+\nabla_\perp\widetilde{\phi}$, where $\omega\equiv(\nabla\times\mathbf{u})_z=-\Delta_\perp\widetilde{C}$, $\Delta_\perp\widetilde{\phi}=-\partial u_z/\partial z$, $\nabla_\perp=\nabla-\mathbf{e}(\mathbf{e}\cdot\nabla)$. Hereafter $\Lambda=0$. Thus, in $\mathbf{k}$ space the velocity $\mathbf{u}$ is given by

$$u_i(\mathbf{k})=(k/k_\perp)^2[e_mP_{im}(\mathbf{k})u_z(\mathbf{k})-i(\mathbf{e}\times\mathbf{k})_i\omega(\mathbf{k})/k^2]. \tag{B1}$$

Multiplying Eq. (B1) for $u_i(\mathbf{k}_1)$ by $u_j(\mathbf{k}_2)$ and averaging over the turbulent velocity field we obtain

$$f_{ij}^{(0)}(\mathbf{k})=(k/k_\perp)^4[f_*f^{(0)}(\mathbf{k})e_{mn}P_{im}(\mathbf{k})P_{jn}(\mathbf{k}) +(\mathbf{e}\times\mathbf{k})_i(\mathbf{e}\times\mathbf{k})_jG^{(0)}(\mathbf{k})/k^4], \tag{B2}$$

where we assumed that the turbulent velocity field in the background turbulent convection is nonhelical. Now we use an identity

$$(k/k_\perp)^2e_{mn}P_{im}(\mathbf{k})P_{jn}(\mathbf{k})=e_{ij}+k_{ij}^\perp-k_{ij}=P_{ij}(\mathbf{k})-P_{ij}^\perp(\mathbf{k}_\perp), \tag{B3}$$

which can be derived from

$$k_z(k_ze_{ij}+e_ik_j^\perp+e_jk_i^\perp)=k_{ij}k^2-k_{ij}^\perp k_\perp^2.$$

Here we also used the identity $(\mathbf{k}_\perp\times\mathbf{e})_i(\mathbf{k}_\perp\times\mathbf{e})_j=k_\perp^2P_{ij}^{(\perp)}(k_\perp)$. Substituting Eq. (B3) into Eq. (B2) we obtain

$$f_{ij}^{(0)}(\mathbf{k})=(k/k_\perp)^2\{f_*f^{(0)}(\mathbf{k})P_{ij}(\mathbf{k}) +[G^{(0)}(\mathbf{k})/k^2-f_*f^{(0)}(\mathbf{k})]P_{ij}^\perp(\mathbf{k}_\perp)\}. \tag{B4}$$

Thus two independent functions determine the correlation function of the anisotropic turbulent velocity field. In the isotropic three-dimensional turbulent flow $G^{(0)}(\mathbf{k})/k^2=f_*f^{(0)}(\mathbf{k})$ and the correlation function reads

$$f_{ij}^{(0)}(\mathbf{k})=f_*W(k)P_{ij}(\mathbf{k})/8\pi k^2. \tag{B5}$$

In the isotropic two-dimensional turbulent flow $G^{(0)}(\mathbf{k})/k^2 \gg f_* f^{(0)}(\mathbf{k})$ and the correlation function is given by

$$f_{ij}^{(0)}(\mathbf{k}) = G^{(0)}(\mathbf{k}) P_{ij}^{\perp}(\mathbf{k}_\perp)/k_\perp^2 . \tag{B6}$$

A simplest generalization of these correlation functions is an assumption that $G^{(0)}(\mathbf{k})/[k^2 f_* f^{(0)}(\mathbf{k})] - 1 = \varepsilon = \text{const}$, and thus the correlation function $f_{ij}^{(0)}(\mathbf{k})$ is given by Eq. (12). This correlation function can be considered as a combination of Eqs. (B5) and (B6) for the three-dimensional and two-dimensional turbulence. When ε depends on the wave vector $\mathbf{k}$, the correlation function $f_{ij}^{(0)}(\mathbf{k})$ is determined by two spectral functions.

Now we derive Eq. (13) for the turbulent flux of entropy. Multiplying Eq. (B1) written for $u_i(\mathbf{k}_2)$ by $s(\mathbf{k}_1)$ and averaging over turbulent velocity field we obtain Eq. (13). Multiplying Eq. (13) by $i(\mathbf{k}_\perp \times \mathbf{e})_i$ we get

$$F^{(0)}(\mathbf{k}) = i(\mathbf{k}_\perp \times \mathbf{e}) \cdot \mathbf{\Phi}_\perp^{(0)}(\mathbf{k}). \tag{B7}$$

Now we assume that $\mathbf{\Phi}_\perp^{(0)}(\mathbf{k}) \propto \mathbf{\Phi}_\perp^* f^{(0)}(\mathbf{k})$. The integration in $\mathbf{k}$ space in Eq. (B7) yields the numerical factor in Eq. (15). Note that for simplicity we assumed that the correlation functions $F^{(0)}(\mathbf{k})$ and $f^{(0)}(\mathbf{k})$ have the same spectrum. If these functions have different spectra, it results only in a different value of a numerical coefficient in Eq. (15).

Now let us discuss the physical meaning of the parameter α. To this end we derived the equation for the two-point correlation function $\Phi_z^{(0)}(\mathbf{r}) = \langle s(\mathbf{x}) \mathbf{u}(\mathbf{x}+\mathbf{r}) \rangle$ of the turbulent flux of entropy for the background turbulent convection [which corresponds to Eq. (14) written in $\mathbf{k}$ space]. Let us rewrite Eq. (14) in the following form:

$$\Phi_z^{(0)}(\mathbf{k}) = (\mathbf{\Phi}^* \cdot \mathbf{e})[k^2 + \Gamma(\mathbf{e} \cdot \mathbf{k})^2] \tilde{\Phi}_w(k), \tag{B8}$$

$$\tilde{\Phi}_w(k) = -(3-\alpha) W(k)/8\pi k^4, \tag{B9}$$

where $\Gamma = 3(\alpha - 1)/(3-\alpha)$. The Fourier transform of Eq. (B8) reads

$$\Phi_z^{(0)}(\mathbf{r}) = (\mathbf{\Phi}^* \cdot \mathbf{e})[\Delta + \Gamma(\mathbf{e} \cdot \nabla)^2] \Phi_w(r), \tag{B10}$$

where $\Phi_w(r)$ is the Fourier transform of the function $\tilde{\Phi}_w(k)$. Now we use the identity

$$\nabla_i \nabla_j \Phi_w(r) = \psi(r) \delta_{ij} + r\psi'(r) r_{ij}, \tag{B11}$$

where $\psi(r) = r^{-1} \mathbf{\Phi}_w'(r)$ and $\psi'(r) = d\psi/dr$. Equations (B10) and (B11) yield the two-point correlation function $\Phi_z^{(0)}(\mathbf{r})$:

$$\mathbf{\Phi}_z^{(0)}(\mathbf{r}) = (\mathbf{\Phi}^* \cdot \mathbf{e}) \left(\psi(r) + r\psi'(r) \frac{1 + \Gamma \cos^2 \tilde{\theta}}{3 + \Gamma} \right), \tag{B12}$$

where $\tilde{\theta}$ is the angle between $\mathbf{e}$ and $\mathbf{r}$. The function $\psi(r)$ has the following properties: $\psi(r=0) = 1$ and $(r\psi')_{r=0} = 0$, e.g., the function $\psi(r) = 1 - (r/l_0)^{q-1}$ satisfies the above properties, where $1 < q < 3$. Thus, the two-point correlation function $\Phi_z^{(0)}(\mathbf{r})$ of the flux of entropy for the background turbulent convection is given by

$$\Phi_z^{(0)}(\mathbf{r}) = (\mathbf{\Phi}^* \cdot \mathbf{e}) \left[1 - \left(\frac{(q-1)(1 + \Gamma \cos^2 \tilde{\theta})}{3 + \Gamma} + 1 \right) \left(\frac{r}{l_0} \right)^{q-1} \right]. \tag{B13}$$

Simple analysis shows that $-3/(q-1) < \alpha < 3$, where we took into account that $\partial \Phi_z^{(0)}(\mathbf{r})/\partial r < 0$ for all angles $\tilde{\theta}$. The parameter α can be presented as $\alpha = [1 + \xi(q+1)/(q-1)]/(1 + \xi/3)$ and $\xi = (l_\perp/l_z)^{q-1} - 1$, where $l_\perp$ and l_z are the horizontal ($\tilde{\theta} = \pi/2$) and the vertical ($\tilde{\theta} = 0$) scales in which the correlation function $\Phi_z^{(0)}(\mathbf{r})$ tends to zero. The parameter ξ describes the degree of thermal anisotropy. In particular, when $l_\perp = l_z$ the parameter $\xi = 0$ and $\alpha = 1$. For $l_\perp \ll l_z$ the parameter $\xi = -1$ and $\alpha = -3/(q-1)$. The maximum value $\xi_{\max}$ of the parameter ξ is given by $\xi_{\max} = q - 1$ for $\alpha = 3$. Thus, for $\alpha < 1$ the thermal structures have the form of column or thermal jets ($l_\perp < l_z$), and $\alpha > 1$ there exist the pancake thermal structures ($l_\perp > l_z$) in the background turbulent convection.

APPENDIX C: THE IDENTITIES USED FOR THE INTEGRATION IN k SPACE

To integrate over the angles in $\mathbf{k}$ space of Eqs. (A30) and (A31) we used the following identities:

$$\int k_{ijmn} d\hat{\Omega} = (4\pi/15) \Delta_{ijmn},$$

$$\int k_{ij} \sin^2 \theta d\hat{\Omega} = (8\pi/15)(2\delta_{ij} - e_{ij}),$$

$$\int k_{ijmn} \sin^2 \theta d\hat{\Omega} = (8\pi/105)(3\Delta_{ijmn} - \Gamma_{ijmn}),$$

$$\int k_{ij}^{\perp} d\hat{\Omega} = 2\pi P_{ij}(\mathbf{e}),$$

$$\int k_{ij}^{\perp} k_{mn} d\hat{\Omega} = (\pi/3)[P_{ij}(\mathbf{e})(\delta_{mn} + e_{mn}) + P_{in}(\mathbf{e}) P_{mj}(\mathbf{e}) + P_{im}(\mathbf{e}) P_{nj}(\mathbf{e})],$$

$$e_j \int k_i^{\perp} k_j k_{mn} k_\perp^{-2} d\hat{\Omega} = (2\pi/3)[P_{in}(\mathbf{e}) e_m + P_{im}(\mathbf{e}) e_n],$$

$$e_j \int k_i^{\perp} k_j k_{mn} k^{-2} d\hat{\Omega} = (4\pi/3)[P_{in}(\mathbf{e}) e_m + P_{im}(\mathbf{e}) e_n],$$

where $P_{ij}(\mathbf{e}) = \delta_{ij} - e_{ij}$, $k_{ijmn} = k_i k_j k_m k_n / k^4$, $d\hat{\Omega} = \sin\theta d\theta d\varphi$, and

$$\Delta_{ijmn} = \delta_{ij}\delta_{mn} + \delta_{im}\delta_{nj} + \delta_{in}\delta_{mj},$$

$$\Gamma_{ijmn} = \delta_{ij} e_{mn} + \delta_{im} e_{jn} + \delta_{in} e_{jm} + \delta_{jm} e_{in} + \delta_{jn} e_{im} + \delta_{mn} e_{ij},$$

$$\gamma_{ijm}=\Delta_{ijmn}e_n=\delta_{ij}e_m+\delta_{im}e_j+\delta_{jm}e_i,$$

$$e_m\gamma_{ijm}=\delta_{ij}+2e_{ij},$$

$$e_n\Gamma_{ijmn}=\gamma_{ijm}+3e_{ijm},\quad e_{mn}\Gamma_{ijmn}=\delta_{ij}+5e_{ij},$$

$$P_{ij}(\mathbf{k})+\varepsilon P^{\perp}_{ij}(\mathbf{k}_{\perp})=(1+\varepsilon)\delta_{ij}-\varepsilon e_{ij}-k_{ij}-\varepsilon k^{\perp}_{ij}.$$

The above identities allow us to calculate the following integrals (which were used for the derivation of equations for the Reynolds stresses and turbulent flux of entropy):

$$\int \tau(k)k_{ij}\Phi^{(0)}_m(\mathbf{k})d\mathbf{k}=(\mathbf{\Phi}^*\cdot\mathbf{e})(\tau_0/30)[15\delta_{ij}e_m+10\alpha e_{ijm}-(2\alpha+3)\gamma_{ijm}+6b_{ijm}],$$

$$\int \tau(k)k_{mn}f^{(0)}_{ij}(\mathbf{k})d\mathbf{k}=(f_*\tau_0/6)[(\varepsilon/4)(\Gamma_{ijmn}-e_{ijmn})-(1/5+\varepsilon/4)\Delta_{ijmn}+(1+\varepsilon)\delta_{ij}\delta_{mn}-(\varepsilon/2)\delta_{ij}e_{mn}-\varepsilon e_{ij}\delta_{mn}],$$

where

$$b_{ijm}=\delta_{ij}(\Phi^*_{\perp})_m+[\varepsilon_{iml}(\mathbf{\Phi}^*\times\mathbf{e})_j+\varepsilon_{jml}(\mathbf{\Phi}^*\times\mathbf{e})_i]e_l,$$

and we used an identity $e_q\varepsilon_{pqn}(\mathbf{\Phi}^*\times\mathbf{e})_m\Delta_{ijmn}=b_{ijp}$.

[1] D. Etling and R.A. Brown, Boundary-Layer Meteorol. **65**, 215 (1993).
[2] B.W. Atkinson and J. Wu Zhang, Rev. Geophys. **34**, 403 (1996).
[3] D.H. Lenschow and P.L. Stephens, Boundary-Layer Meteorol. **19**, 509 (1980).
[4] J.C.R. Hunt, J. Fluid Mech. **138**, 161 (1984).
[5] J.C. Wyngaard, J. Atmos. Sci. **44**, 1083 (1987).
[6] J.C.R. Hunt, J.C. Kaimal, and J.I. Gaynor, Q. J. R. Meteorol. Soc. **114**, 837 (1988).
[7] H. Schmidt and U. Schumann, J. Fluid Mech. **200**, 511 (1989).
[8] R.I. Sykes and D.S. Henn, J. Atmos. Sci. **46**, 1106 (1989).
[9] L. Mahrt, J. Atmos. Sci. **48**, 472 (1991).
[10] S.S. Zilitinkevich, *Turbulent Penetrative Convection* (Avebury Technical, Aldershot, 1991), and references therein.
[11] A.G. Williams and J.M. Hacker, Boundary-Layer Meteorol. **61**, 213 (1992); **64**, 55 (1993).
[12] A.G. Williams, H. Kraus, and J.M. Hacker, J. Fluid Mech. **53**, 1187 (1996).
[13] S.S. Zilitinkevich, A. Grachev, and J.C.R. Hunt, in *Buoyant Convection in Geophysical Flows*, edited by E. J. Plate *et al.* (Kluwer Academic, Dordrecht, 1998), pp. 83–113.
[14] G.S. Young, D.A.R. Kristovich, M.R. Hjelmfelt, and R.C. Foster, Bull. Am. Meteorol. Soc. **83**, 997 (2002).
[15] R. Krishnamurti and L.N. Howard, Proc. Natl. Acad. Sci. U.S.A. **78**, 1981 (1981).
[16] M. Sano, X.Z. Wu, and A. Libchaber, Phys. Rev. A **40**, 6421 (1989).
[17] S. Ciliberto, S. Cioni, and C. Laroche, Phys. Rev. E **54**, R5901 (1996).
[18] S. Ashkenazi and V. Steinberg, Phys. Rev. Lett. **83**, 3641 (1999); **83**, 4760 (1999).
[19] L.P. Kadanoff, Phys. Today **54**(8), 34 (2001).
[20] J.J. Niemela, L. Skrbek, K.R. Sreenivasan, and R.J. Donnelly, J. Fluid Mech. **449**, 169 (2001).
[21] E.D. Siggia, Annu. Rev. Fluid Mech. **26**, 137 (1994).
[22] E.W. Bolton, F.H. Busse, and R.M. Clever, J. Fluid Mech. **164**, 469 (1986).
[23] A.S. Monin and A.M. Yaglom, *Statistical Fluid Mechanics* (MIT Press, Cambridge, MA, 1975), and references therein.
[24] A.D. Wheelon, Phys. Rev. **105**, 1706 (1957).
[25] G.K. Batchelor, I.D. Howells, and A.A. Townsend, J. Fluid Mech. **5**, 134 (1959).
[26] G.S. Golitsyn, Dokl. Acad. Nauk **132**, 315 (1960) [Sov. Phys. Dokl. **5**, 536 (1960)].
[27] H.K. Moffatt, J. Fluid Mech. **11**, 625 (1961).
[28] J.L. Lumley, Phys. Fluids **10**, 405 (1967).
[29] J.C. Wyngaard and O.R. Cote, Q. J. R. Meteorol. Soc. **98**, 590 (1972).
[30] S.G. Saddoughi and S.V. Veeravalli, J. Fluid Mech. **268**, 333 (1994).
[31] T. Ishihara, K. Yoshida, and Y. Kaneda, Phys. Rev. Lett. **88**, 154501 (2002).
[32] S.A. Orszag, J. Fluid Mech. **41**, 363 (1970), and references therein.
[33] W.D. McComb, *The Physics of Fluid Turbulence* (Clarendon, Oxford, 1990).
[34] A. Pouquet, U. Frisch, and J. Leorat, J. Fluid Mech. **77**, 321 (1976).
[35] N. Kleeorin, I. Rogachevskii, and A. Ruzmaikin, Sov. Phys. JETP **70**, 878 (1990); N. Kleeorin, M. Mond, and I. Rogachevskii, Astron. Astrophys. **307**, 293 (1996).
[36] I. Rogachevskii and N. Kleeorin, Phys. Rev. E **61**, 5202 (2000); **64**, 056307 (2001).
[37] P.N. Roberts and A.M. Soward, Astron. Nachr. **296**, 49 (1975).
[38] N. Kleeorin and I. Rogachevskii, Phys. Rev. E **50**, 2716 (1994).